Temperature Dependence Of The Transient Characteristics in NPT IGBT Using Linear and Parabolic Model

A thesis submitted in partial fulfillment of the requirements
for the degree of Bachelor of Science
in the
Department of Electrical and Electronic Engineering

Submitted by-

Shoulin Tania – 12310008

Dipraj Saha – 12121123

Fahmida Faiza – 12121036

BRAC University
Fall 2016

Declaration

This is to declare that this thesis named "Temperature Dependence Of The Transient Characteristics in NPT IGBT Using Linear and Parabolic Model" is submitted by the authors listed for the degree of Bachelor of Science in Electrical and Electronics Engineering to the Department of Electrical of Electronics Engineering under the School of Engineering and Computer Science, BRAC University. We hereby affirm that the research work and result was conducted solely by us and no other. Materials of the study and work found by other researchers have been properly referred and acknowledged. This thesis paper, neither in whole nor in part, has been previously submitted elsewhere for appraisal.

Submission Date: 14th December, 2016.

_____
Shoulin Tania

_____
Famida Faiza

_____
Dipraj Saha

Abstract:

To be considered as an efficient assistant, power semiconductor devices are being used in many power converter applications and technologies, particularly with high variable loads. In this regard, monitoring temperature of the device junction is indispensable. In this literature review, the characteristics of Non Punch Through (NTP) Insulated Gate Bipolar Transistor (IGBT) during the turn off state has been analyzed with the change in temperature in different carrier lifetimes. Moreover, the anode voltage, anode current, carrier charge and power loss characteristics of IGBT is shown by comparing the ideal linear model and parabolic model with temperature variance.

Acknowledgement

We convey our sincere gratitude to our supervisor, Avijit Das, Lecturer, BRAC University for uplifting and providing us the valuable guidance to complete this research. . He has provided us with the necessary materials & instructions which greatly helped us a lot to understand the topic & analyze it better. He has always been there for us to rescue in case of any problems that we might encounter while dealing with this issue. Without his keen supervision, it was virtually impossible for us to finish this report successfully in time. We are grateful to all of our peers and every other individual who has supported, encouraged and lent us hand whenever it was required throughout our research.

Again, we would like to thank our parents for the continuous support and encouragement which makes us complete the work.

Finally, we are very grateful to the Almighty Allah, who has blessed us with knowledge and ability to write this report successfully.

Contents:

List of Figures :

List of Tables :

Abbreviations:

IGBT	Insulated Gate Bipolar Transistor
BJT	Bipolar Junction Transistor
MOSFET	Metal Oxide Semiconductor Field Effect Transistor
VDMOSFET	Vertical Double Diffused MOSFET
RK4	4^{th} Order Runga Kutta Method

Physical Parameter:

Ambipolar Diusivities, D	18 cm^2/s
Supply voltage, V_{bus}	400 V
Dielectric constant of Si , $\in_{si}$	11.7*8.854*10^-14 F/cm
Charge of electron	1.6 * 10^-19 C
Base doping concentration	2*10^14 cm^{-3}
Hole Diffusivity	14 cm^2/s
Metallurgical base width	9.3* 10^- 3 cm

Device active area	.1 cm^2
Emitter electron saturation current	6*10 ^-14 A
ntrinsic carrier concentration	1.45 * 10^10 cm^{-3}
Electron mobility	1500 cm^2/Vs
Hole mobility	450 cm^2/Vs
Ambipolar mobility ratio	3.3
Total current	10 A

Symbols:

A	Device Active area	cm^{-3}
I_n, I_p	Electron Hole Current	A
δp	Excess Carrier Concentration	cm^{-3}
n, p	Electron, hole carrier concentration	cm^{-3}
Q	Total Excess Carrier Base Charge	C
Q_0	Steady State Base Charge	C
P_0	Excess Carrier Concentration	cm^{-3}
$\emptyset n, \emptyset p$	Electron, hole quasi-fermi potential	V
E	Electric Field	V/cm
$\in_{Si}$	Dielectric constant of Si	F/cm

Q	Electron Charge	C
$\mu n, \mu p$	Electron, hole mobility	cm^{-2}/Vs
D_n, D_p	Electron, hole diffusivity	cm^{-2}/s
T_{HL}	High level excess carrier lifetime	s
$I_T = I_n + I_p$	Total Current	A
$b = \frac{\mu n}{\mu p}$	Ambipolar mobile ratio	-
D	Ambipolar Diffusivity	Cm
L	Ambipolar Diffusion Length	Cm
x	Distance in Base from Emmiter	Cm
W_B	Metallurgical base width	cm
W	quasi-neutral base width	cm
W_{bcj}	base-collector depletion width	cm
C_{bcj}	collector-base depletion capacitance	F
N_B	base doping concentration	cm^{-3}
V_{CE}	built-in potential of base-collector junction	V
I_{sne}	emitter electron saturation current	A
V_T	Mosfet channel thrershold voltage	V

Chapter 1
Introduction

An Insulated-Gate Bipolar Transistor (IGBT) is a three-terminal power semiconductor device which is a combination of the characteristics of power MOSFET Input and bipolar transistor. AsIGBT is a minority carrier device with high input impedance and large bipolar current carrying capability, it was initially used as an electronic switch with efficiency and fast switching. The internal voltage drop of a bipolar transistor in its turn on state is less than that in a power MOSFET with comparable current and blocking voltage. On the other hand, a MOSFET can be turned on at the gate with less energy than a bipolar transistor, which requires a relatively high current that has to be maintained throughout the on period. That's why IGBT is a functional integration of Power MOSFET and BJT devices in monolithic form. The IGBT is also a three terminal (gate, collector, and emitter) full-controlled switch. Its gate/control signal takes place between the gate and emitter, and its switch terminals are the drain and emitter. It is a combination of the low on state resistance of power bipolar transistor and the high input impedance of power MOSFET gave a major advantage where the high impedance allows controlled turn-on and gate controlled turn off.[3]

However, IGBT is preferable in many applications in power electronics area, specifically in Pulse Width Modulated (PMW) servo and the three-phase drives requiring high dynamic range control and low noise. Furthermore, it switches electric power in many modern appliances: variable frequency drives (VFDs), electric cars, trains, variable speed refrigerators, Uninterruptible Power Supplies (UPS), lamp ballasts, air-conditioners and even stereo systems with switching amplifiers. Since it is designed to turn on and off rapidly, amplifiers that use it often synthesize complex waveforms with pulse-width modulation and low-pass filters. In switching applications, modern devices feature pulse repetition rates well into the ultrasonic range-frequencies which are at least ten times the highest audio frequency handled by the device when used as an analog audio amplifier.

However, a MOSFET can be turned on at the gate with less energy than a bipolar transistor, which requires a relatively high current that has to be maintained throughout the on period.

That's why IGBT is a functional integration of Power MOSFET and BJT devices in monolithic form. The IGBT is also a three terminal (gate, collector, and emitter) full-controlled switch. Its gate/control signal takes place between the gate and emitter, and its switch terminals are the drain and emitter.

The main advantages of IGBT over a Power MOSFET and a BJT are [4]

- Due to havingconductivity modulation and superior on-state current density, it has a very low on-state voltage drop. So smaller chip size is possible and the cost can be reduced.
- It has lower on-state and switching losses and also lowers thermal impedance.
- Low driving power and a simple drive circuit due to the input MOS gate structure. It can be easily controlled as compared to current controlled devices (thyristor, BJT) in high voltage and high current applications.
- Wide SOA: It has superior current conduction capability compared with the bipolar transistor. It also has excellent forward and reverse blocking capabilities.

The major limitations are:

- A reduction in on-state voltage can cost the IGBT to experience slower switching speed at turn-off. The reason is that while electron flow can be abruptly halted simply by reducing the gate-emitter voltage below the gate threshold voltage (as is the case with the MOSFET), there's still the matter of the holes that are left in the drift and body regions (there's no terminal connection to remove them). The only way to get them out of there is by sweep-out, which is dependent upon voltage across the device and internal recombination. As a result, the device displays a tail current at turn-off until the recombination is complete. This has always been a big drawback for the IGBT.
- Switching speed is inferior to that of a Power MOSFET and superior to that of a BJT. The collector current tailing due to the minority carrier causes the turn-off speed to be slow.
- There is the possibility of latch-up due to the internal PNPN thyristor structure.

Several models have been Parabolic in the literature to describe both the DC and the transient

behaviors of the IGBT. These models can be classified into two categories: physics-based and behavioral (compact) models.

The model outlined in this thesis dissertation belongs to the category of physics based models in that the basic semiconductor physics of the IGBT device is used to develop relations between the excess minority carrier's distribution, the anode current(IT), the base current and the output voltage of the device (V=VCE=VBC). There are no exact solutions when considering physics based modeling approach. Appropriate mathematical representations should be found to roughly approximate the solution. It is possible to reach an exact solution if certain assumptions are met when considering the imposed boundary conditions. The analytical modeling approach uses parameters, which have physical meanings and are related to each other based on the device physics. However, advancinging a physical model is time consuming. Since there are some simplifying approximations made when developing a physics-based model, accuracy may not be 100%. Additionally, new device or different structural IGBT needs some new model or modifications.

The analytical model developed by Hefner et al. [1-4] is the most complete in the section of physics-based IGBT model. The general ambipolar transport electron is $In\ (t)$ which was used to find an expression for the voltage, $dV\ (t)/dt$. Hefner used the expression of displacement current $In\ W(t)$ to obtain V(t) for the transient operation of IGBT. Hefner implemented the concept of moving the redistribution current. In transient approach Hefner neither used the steady state expression for p(x) nor did linearize the steady state expression for
p(x). Moreover Hefner assumed C_{bcj}(t) to be constant with time, which is not so in reality.

Trivedi et al. [5] provided a numerical solution to obtain voltage, ($dV\ (t)/dt$) in terms of the total current I_T during the turn-off for hard and soft switching IGBT application. The sweeping out action of the excess carriers in the drift region due to the widening of the collector-base depletion was used to obtain $dV\ (t)/dt$ expression. Since W(t) shrinks due to the widening of the depletion region in the collector-base, the charges are forced to be taken away and I_h= qp(X)v(X) = qp(X)dW(t)/dt .

Ramamurthy et al. [6] provided an analytical expression for the voltage variation with time $dV(t)/dt$ for the turn-off of the IGBT. The simple expression for the variation of the internal charges and the boundary conditions with voltages is a non-linear one. For the turn- off analysis, Ramamurthy linearized the steady state carrier concentration expression p(x).
Ramamurthy used a positive value for $d(t)/dt$ instead of a negative sign, which contradicts the equality $W(t)= W_B-W_{bcj}(t)$.

Fatemizadeh et al. [7] developed a semi-empirical model for IGBT in which the DC and the transient current transport mechanisms of the device were approximated by simple analytical equations. The model equations of the IGBT were installed on the PSPICE simulator using analog behavioral modeling tools. However, the accuracy of the model is limited by the fact that the analytical semi-empirical model is over simplified.

Yue et al. [8] presented an analytical IGBT model for the steady state and transient applications including all levels of free carrier injection in the base region of the IGBT. The authors have shown that the low and high injection models significantly overestimate the IGBT current at large and small bias conditions respectively.

Kraus et al. [9] considered an NPT IGBT with a higher charge carrier lifetime and lower emitter efficiency. The injection of electrons into the emitter of the IGBT instead of carrier recombination in the base determined the I-V characteristics. The anode hole currents and the emitter hole currents are assumed constant. Due to his neglecting of the recombination in the base, a linear charge distribution instead of the hyperbolic function was derived.

Kuo et al. [10] derived an analytical expression for the forward conduction voltage (*VF*) for NPT and PT IGBTs taking into account the conductivity modulation in the base of the IGBT.
The MOSFET section has not been included in the analysis. Since IMOS controls the turn-off process of the IGBT, the MOSFET section should have been included.

Sheng et al. [11] solved the two dimensional (2-D) carrier distribution equations to model the forward conduction voltages, which can be used in circuit simulation and device analysis for (DMOS IGBT). The drawback of this modeling approach is that it contains complex terms that would impose some requirements on the simulator.

Sheng et al. [12] reviewed IGBT models published in the literature; he then analyzed, compared and classified models into different categories based on mathematical type, objectives, complexity and accuracy. Although [14] claimed that many mathematical models are accurate and able to predict electrical behavior in different circuit conditions compared to the behavioral models, it failed to provide a comprehensive physical model for understanding the device mechanisms.

Leturcq [13] showed a simplified approach to the analysis of the switching condition in IGBT. The approach was based on a new method for solving the ambipolar diffusion equation taking the moving depletion boundary in the base into consideration. This paper helped in understanding the switching process in IGBT.

The above literature survey dealt mainly with IGBT having planar structures, namely the Non-Panch Through (NPT) and the Punched Through (PT) IGBT, although other structures were parabolic in the literature to improve the I-V characteristics of IGBTs, temperature operation or develop better physics-based models.

Chapter 2 describes the basic structure of an IGBT and provides a description of the IGBT operation. In addition, the chapter introduces the ambipolar transport analysis, which is the key feature in modeling the IGBT device. The conclusion of the chapter highlights the basic tools for the analysis: the steady state and the transient operation of an IGBT. Chapter 3 covers the literature review analysis of the most important transient modeling of IGBT. Chapter 4 introduces the parabolic physics-based model for NPT IGBT wherein the steady state part of the model is derived by solving the ambipolar diffusion equation in the base. The turn-off transient part of the model is based on the availability of a new expression for excess carrier charge distribution in the base. The transient voltage is obtained numerically from this model. In chapter

5, we have showed the changes in characteristics of anode voltage, current and power dissipation with respect to temparature with figures. Chapter 6 covered our limitations and future work of this analysis.

Chapter 2

About IGBT

IGBT is a switching device combine with BJT and MOSFET, so in struscture as well as operation, the combination of BJT and MOSFET can be seen. This chapter will cover IGBT's basic structure and operation.

2.1 Standard Structure

2.1.1 Cross sectional structure

A structured IGBT has main three parts, Gate, Emmiter and Collector. In the cross section of IGBT, different layers are present which are shown in the below figure. It can be compared with the vertical double diffused MOSFET. The difference between them is that in IGBT, a heavily doped p-type substrate is placed in lieu of a highly doped n-type drain contact in the VDMOSFET. In reverse bias mode, a high blocking voltage used to create. To support that, a lightly doped but thick n-type epitaxial layer ($N_B = 10^{14} cm^{-3}$) is placed up of the p-type substrate. A highly doped p-type region ($N_A = 10^{19} cm^{-3}$) is also present in the structure to prevent the activation of the PNPN thyristor when the device operates. The gate of IGBT is very simple circuit which has beenn taken from power MOSFET. As power MOSFET is a voltage controlled device, so little input gate current can operate the device. In IGBT, small gate input current operates the device and it is easy to use for simple design.

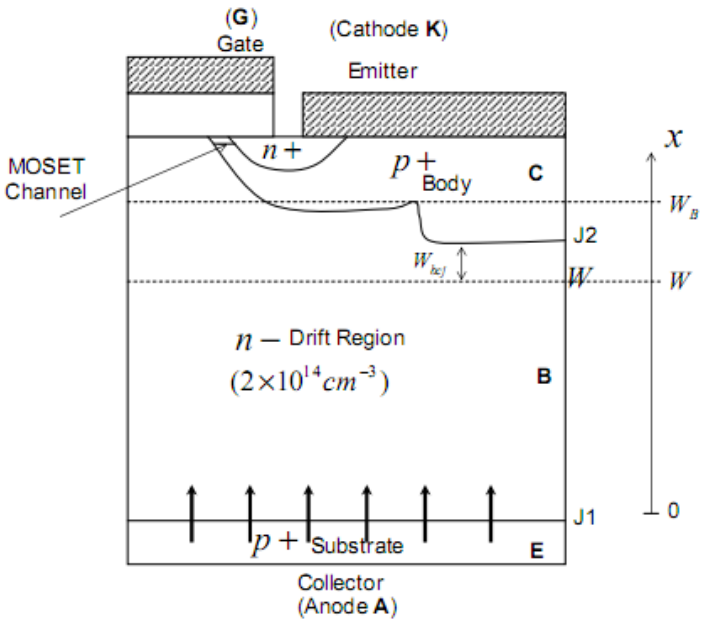

Figure 2.5: A cross sectional structure of the IGBT half-cell [14]

2.1.2 NPT and PT IGBT

Based on the presense of an extra highly doped n+ buffer layer, there are two kinds of IGBT, one is PT (Punch Through) and other one is NPT (Non-Punch Through). The PT IGBT is with the extra n+ buffer layer and without this layer, that called NPT IGBT. The difference between them is showed in Figure 2.2.

The PT IGBT has an extra n+ buffer layer than the other kind. This layer is placed on P+ Substrate layer. Because of the presense of this layer, the J1 junction gets gets a punch through from the J2 junction. This layer also acts as a shield to the J1 junction. But during the on state (turn-on) operation, total charges did not get enough space because of an extra n+ buffer layer. So, in the time of switching, the n+ layer removes charges more quickly. This layer acts as a recombination hub where holes and electrons get recombined before the holes get the time to reach the base region. For this, some lower efficiency holes will be injected into the base region. Because of this, carrier lifetime of the holes are reduced and switching frequency is increased. The amount of injected holes in the base region is less than the NPT IGBT, so the on-state

voltage is increased in PT IGBT but the conductivity modulation(higher base resistance) is reduced. But the increased on-state voltage acts negetively to the reduced turn-off time.

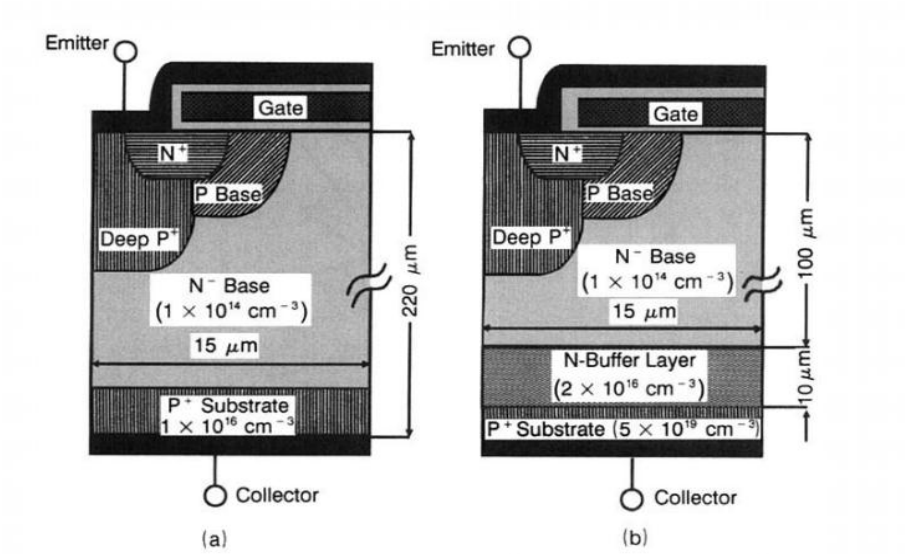

FIGURE 6.2: Cross section structure of (a) NPT IGBT and (b) PT IGBT [15]

In this thesis, NPT IGBT is studied. NPT IGBT has no n+ buffer layer, so the n- layer of base region is more thick than the PT IGBT. For the thickness, NPT IGBT has high resistance and when the J2 junction is reverse biased, higher reversed voltage can be uninterrupted. As a result, J2 junction does not punched through to J1 junction, means a non-punch through situation created. If the punch through happened, the device will more likely to break down as the breakdown voltage of IGBT is depraved. When J1 junction is forward biased and gate voltage exceeds the threshold voltage, p+ substrate will inject more holes. These injected holes density arises slowly and when it crosses the background doping(N_B) density, the resistance of n-layer is shortened. In NPT IGBT, the turn-off time is more long than PT IGBT as the removal of so many stored charges in the base region is slow because of less recombination centers. As carriers are not used to recombine fastly, the carrier lifetime increases. In NPT IGBT, the amount of injected charges from p+ layer to n- is larger than PT IGBT and the injected holes do not recombine very fast as PT IGBT. The NPT IGBT has equal forward and reverse breakdown voltage, so it is totally fit for AC applications. PT IGBT's has greater forward breakdown voltage than reverse breakdown voltage, for this it fits to DC circuits where devices do not need

support voltage in reverse direction. Fig.2.3 shows Doping Concentration and Electric Field distribution between NPT and PT IGBT.

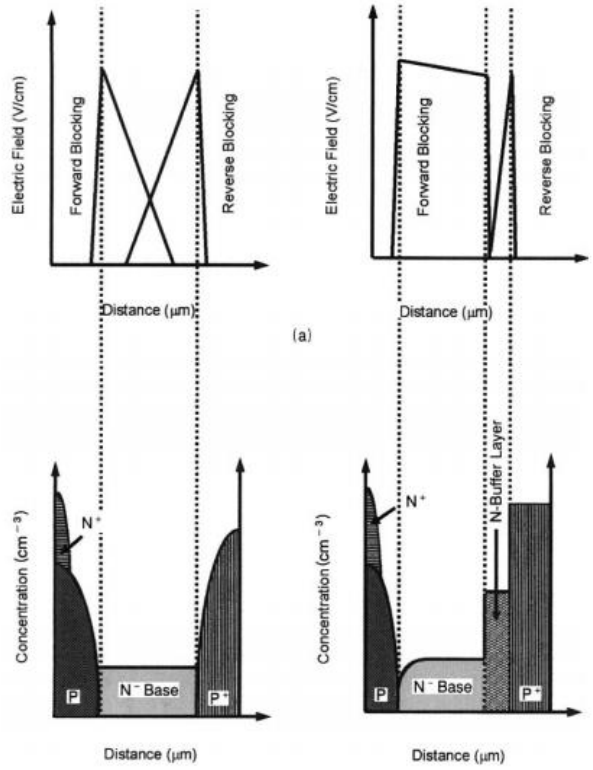

FIGURE 2.3: Doping Concentration & Electric Field Distribution (a) NPT IGBT & (b) PT IGBT [15]

Table 2.1: Comparison of NPT and PT IGBT characteristics

Parameter	NPT	PT
Switching loss	Medium	Low
Conduction loss	Medium	Low
Paralleling	Easy	Difficult
Short circuit test	Yes	Limited; high gain

2.2 Principles of operation of IGBT

2.2.1 Equivalent circuit of IGBT

An equivalent circuit has been figured on the basis of the standard structure which has been shown in Fig. 2.4.

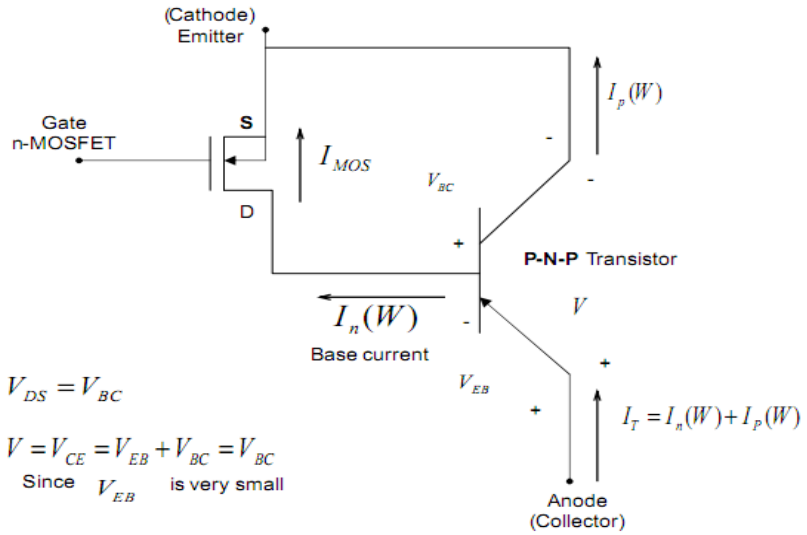

FIGURE 2.4: The equivalent circuit model of IGBT [14]

The structure has two parts, one is PNP transistor (BJT) and a n channel MOSFET. The PNP transistor consists of p+ substrate, n-epilayer and p+ base. In the IGBT, the p+ substrate acts as an emitter of BJT and also the anode terminal of the device. When the p+ substrate is forward biased (V_{EB}> 0), the transistor current, I_T produced by the minority carrier injection and it flows from anode region. This transistor current has two parts at the base. Those are-

- Electron Current- In(W)
- Hole Current- Ip(W)

The Cathode voltage, V_{AC} is-

$$V_{AC} = V_{EB} + V_{BC}$$

Where,

V_{EB}=Bipolar Emitter to Base voltage.

V_{BC}=Base to Cathode voltage.

Basically V_{DS} of MOSFET & V_{BC} are same. Since V_{EB} is very small, we can consider

$$V_{AC} = V_{BC}$$

From the design of the equivalent circuit of IGBT, a circuit symbol can also be created which is shown in Fig. 2.5.

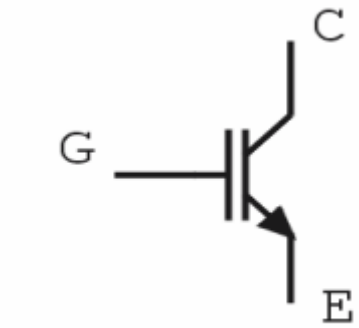

FIGURE 2.5: Circuit symbol of IGBT [14]

The circuit symbol of IGBT has three parts. These are-

Collector (C) - Anode terminal of IGBT.

Gate (G) - Gate terminal of MOSFET.

Emitter (E) - Cathode terminal of IGBT.

2.2.2 IGBT Operation

In the Gate terminal of IGBT, a positive voltage is applied. When the gate voltage is greater than threshold voltage(V_T), electrons flows to the surface under the gate and these electrons changed

the p+ body region into an n channel. This channel is created between n^+ source and n^- drift region.

In the anode terminal of the IGBT, when a positive voltage applied, the collector of the IGBT is lower voltage than emitter. In the emitter section (p+ region), the holes (minority carriers) are injected and the holes flows to the base region (n^- drift region). Through the injected holes, the positive bias of emitter terminal is increased as well as the concentration of holes. As time passes by, the concentration of holes goes beyond the background doping level of the n-drift region. These carriers degrades the resistance of the n- drift region, so the holes recombined with electrons respectively and produces anode current (on state).

On the other hand, if a negetive voltage is applied in the anode terminal, the emitter-base junction will become reverse biased and current will be near zero. The depletion region will widen into the n-drift region and as a result a large voltage drop will occur.

In IGBT, switching operation is done by MOSFET gate voltage. When the gate voltage becomes less than threshold voltage, the turn-off occurs. In this time, the channel that created to pass the charges will be off and no electron current will be present in the MOSFET channel. In the mean time, the holes those were stocked during the on state situation, removes by the time being.

Based on the time that charges which were stored during the turn-on state of IGBT, needs to be removed from the n-drift region, the switching speed of IGBT is measured.

2.3 Basic Tools for Operation

To describe the operation of IGBT, one Physics-based modeling approach is considered. The points considered for the operation are as below-

- In the IGBT n-drift region, the carrier distribution is described by the ambipolar diffusion equation because of the high level injection of holes in this region ($p(x) >> N_B$).

$$\frac{\partial^2 p(x)}{\partial x^2} = \frac{p(x)}{L^2} + \frac{1}{D}\frac{\partial \mathrm{p(x)}}{\partial \mathrm{x}}$$

Here,

N_B = Base background doping concentration

$p(x)$ = Hole concentration

$L = \sqrt{D\tau_{HL}}$, $\tau_{HL} = 5 \times 10^{-7}(\frac{T}{300})^{1.5}$

- Transport of the bipolar charge is assumed to be one-dimensional (1-D) for the ease of analysis.
- The emitter region of the BJT part of the IGBT which acts like the recombination centers for minority carriers (electrons)from the lightly doped areas, has a very high doping concentration level ($p^+ >> 10^{18} cm^{-3}$)
- The depletion region of minority carriers' space charge region, supports the entire voltage drop across the collector-base terminals based on Poisson's equation. But the effect of mobile carriers in the depletion region is not clarified in this thesis dissertation.
- The τ_{HL} is being changed with temparature, so related parameters like anode voltage and current characteristics will also change.

2.3.1 The Steady State Operation

For the steady state operation of the NPT IGBT, the equivalent circuit model and the 1-D coordinate system is used. The 1-D coordinate system is showed in Fig. 2.6. In this figure, IGBT total current is I_T, hole current is Ip of the BJT and base or MOS electron current is I_n.

I_T can be expressed in other ways:

$$I_T = I_p(x = 0) + I_n(x = 0) \quad (2.1)$$

$$I_T = I_p(x = W) + I_p(x = W) \quad (2.2)$$

$$I_T = I_p(x) + = I_n(x) \qquad (2.3)$$

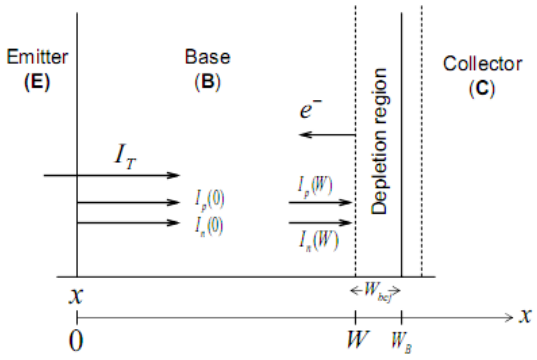

FIGURE 2.6: 1-D coordinate system used in the modeling of the NPT IGBT [14]

The IGBT operation is done under low gain and high level injection case. The current equations are-

$$J_n = nq\mu_n + qD_n \frac{\partial n(x)}{\partial x} \qquad (2.4)$$

$$J_n = pq\mu_p - qD_p \frac{\partial p(x)}{\partial x} \qquad (2.5)$$

Here, J_n is the electron current & J_p is the hole current.

Here, whole J_n and J_p is affected by temparature by a simple equation. The below table will show the changes in various terms of IGBT operation regarding temparature.

Table 2.3.1: Equations describing temparature dependence of various semiconductor properties in Silicon.[16]

Parameter	Temperature Dependence Equation
Carrier lifetime	$\tau_{HL} = 5 \times 10^{-7}\left(\frac{T}{300}\right)^{1.5}$
Electron mobility	$\mu_n = 1400\left(\frac{300}{T}\right)^{2.5}$
Hole mobility	$\mu_p = 450\left(\frac{300}{T}\right)^{2.5}$
Intrinsic concentration	$n_i = 3.88\times10^{16}(T)^{1.5} \Big/ \exp\left(\frac{7000}{T}\right)$

The first terms of the equations indicates the drift component and the second terms are indicates the diffusion component.

If the excess carrier concentration is greater than the background concentration, the transferring of electrons and holes are coupled by the electric field in the drift region in terms of the transport equations. The minority carrier current density J_n cannot be neglected and ends up affecting the majority carrier current density J_p. Hence equations 2.4 & 2.5 cannot be separated.

So Jp and Jn created the total current density. It can be written as,

$$J_T = J_n + J_p$$

$$= \left(nq\mu_n + pq\mu_p\right)E + q\left(D_n\frac{\partial n(x)}{\partial x} - D_p\frac{\partial p(x)}{\partial x}\right)$$

Substituting the electric field from the above equation and put into equation (2.4) gives

$$J_n = \left[\frac{nq\mu_n}{nq\mu_n + pq\mu_p}\right]J_T + q\frac{\partial n}{\partial x}\left[\frac{nq\mu_n D_P + pq\mu_p D_P}{nq\mu_n + pq\mu_p}\right]$$

An ambipolar diffusion coefficient D is specified as

$$D = \left[\frac{nq\mu_n D_P + pq\mu_p D_P}{nq\mu_n + pq\mu_p}\right]$$

So Jn can be written as

$$J_n = \left[\frac{b}{1+b}\right] J_n + qD\frac{\partial n}{\partial x} \qquad (2.6)$$

Here, b $= \frac{\mu_n}{\mu_p}$

Repeating the same procedure in the equation (2.6) and J_p is as followed,

$$J_p = \left[\frac{b}{1+b}\right] J_T - qD\frac{\partial p}{\partial x} \qquad (2.7)$$

Here, J_T is the total current density

$$J_T = J_n + J_p \quad [\text{assuming } n=p]$$

By solving the steady state hole continuity equation, the equation for Excess Hole Carrier Distribution, p(x) can be get,

$$\frac{\partial^2 p(x)}{\partial x^2} = \frac{p(x)}{L^2} \qquad (2.8)$$

From the coordinate system mentioned in Fig. 2.1, the boundary conditions for the excess hole carrier distribution can get. These are,

$$p(x=0) = P_0 \qquad (2.9)$$

$$p(x=W) = 0 \qquad (2.10)$$

Equation (2.10) indicates that for forward condition, the collector-base junction being reversed biased and equation (2.10) also indicates that emitter-base junction is forward biased.

Here,

P_0 is the excess carrier concentration at x=0,

W(t) is the quasi-neutral base width which is

$$W = W_B - W_{bcj} \qquad (2.11)$$

Here, W_B is the metallurgical base width and W_{bcj} is the collector-base depletion width. Poisson's equation is

$$\frac{d^2V}{dx^2} = \frac{qN_B}{\epsilon_{Si}} \qquad (2.12)$$

From Poisson's equations, one expression for the collector-base junction depletion width can be ,

$$W_{bcj} = \sqrt{\frac{2\epsilon_{Si}V_{bc}}{qN_B}}$$

Here,

N_B = Doping concentration of the lightly doped region of the IGBT

ϵ_{Si} = Dielectric constant of silicon.

V_{bcj} = Junction Voltage(V)

$= V_{bc} + V_{bi}$

The junction voltage is the collector-base junction voltage drop of the BJT part of the IGBT and V_{bi} is the built in potential. Now, from figure 2.6

$$W = W_B - \sqrt{\frac{2\epsilon_{Si}V}{qN_B}}$$

Here,

$V = V_{bc} = V_{BE} = V_A$ = collector-base voltage appears across the drift region.

2.3.2 Transient Operation of IGBT

The IGBT switching is fast because of the quick turn-on time. But the turn-off time is slow due to the open base of PNP transistor on turn-off time. In Fig. 2.7, the turn-off transient characteristics of IGBT is showed where I_T (0^+) is the current after the initial rapid fall. The initial drop in the anode current caused by the sudden removal of the MOS channel. As the lightly doped n- layer stored the carriers, a slower decay can be seen. When the gate voltage goes under the threshold voltage, turn-off process started. At this time, the channel for passing the electron is closed, so the MOS current I_{MOS} becomes zero.

$$I_{MOS} = I_n(W) = 0$$

As a result, the depletion region at the n- (base-collector side or source of MOSFET) is widened with respect to the increasement of collector-base voltage, V_{bc}.

Current $I_T(0^-)$ and $I_T(0^+)$ is related by β_{tr}. This β_{tr} is the ratio of the current immediately after the initial rapid fall to the magnitude of the fall and is shown along with the ratio of W(t) to *L (W(t)/L)* in the appendices.

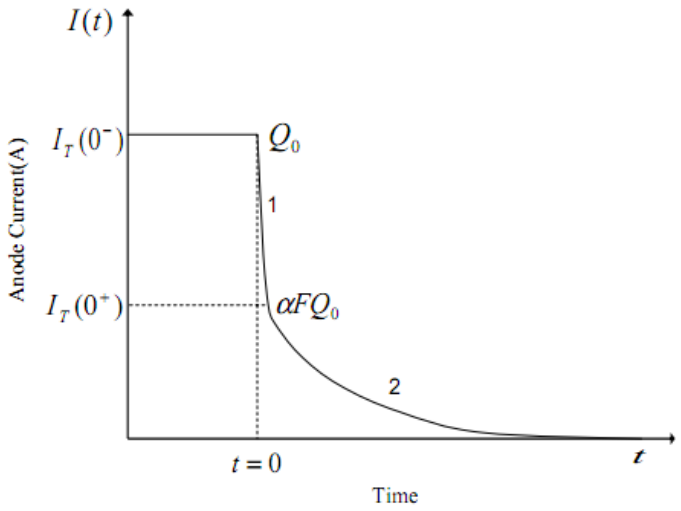

FIGURE 2.7: Typical IGBT turn-off transient showing turn-off phases (1 & 2) [14]

In the second period of the turn-off period transient, some losses occurs. These losses are the main element of switching loss of IGBT. The second phase is slower than other phases because of the higher time required removing or extracting the injected carriers. This high switching losses is considered as one of the supreme drawback of IGBT. The consecuences of this drawback can be solved by lowering the lifetime of the carriers in the base through recombination of extraction processes as fastly as possible before the device reaches its blocking voltage state.

IN the period of turn-off, the collector-base junction is reversed biased and its depletion region widens. At the period of on-state of IGBT, the base-collector junction is reverse biased that showed in Fig. 2.4. When the IGBT is off, the base-collector junction is remains reversed biased

and V_{bc} is increased and also helps the depletion region to increase since the current decreases. This increased depletion region supports the entire voltage drop across the device as mentioned earlier on the basis of Poisson's equation. As the quasi-neutral base width(W(t)) of the IGBT changes with time and decreases with the increase of $V_{bc.}$, an expression for the rate of rise of the voltage across the device$\frac{dV(t)}{dt}$(varying ofthe output voltage) during the switching-OFF of the IGBT from the collector-base junction depletion width W_{bcj} can be derived. If equation 2.11 and 2.13 is marzed, a time derivative of $W_{bcj}(t)$ can get.

$$\frac{dW_{bcj}(t)}{dt} = \sqrt{\frac{\in_{Si}}{2qN_{BV(t)}}}\frac{dV(t)}{dt}$$

The above equation shows the time rate of the change of the quasi-neutral base width (W(t)) that covers almost all the length across the drift region during the turn-off since the collector-base junction is reversed biased.

Chapter 3

Literature review of some transient modeling of IGBT:

Several models have been Parabolic in the literature to describe both the DC and the transient behaviors of the IGBT. In this section, we have reviewed the most popular Parabolic model by Allen R. Linear.

3.1 Approach Taken By Allen R. Hefner

3.1.1 Expression for transient voltage & stored charge decay

In Linear's [1] [2] transient modeling approach, the general ambipolar trans-port electron current expression

$$I_n(W(t)) = \frac{I_T(t)}{1+\frac{1}{b}} + qAD\frac{\partial n(x,t)}{\partial x}$$

This expression was used to find an expression for the voltage rise (dV(t)/dt). $I_n(W(t)) = I_{MOS}$ as shown in Fig. 2.6 and it is important since it controls the operation of IGBT.

Since the reverse bias on junction J_2 in Fig. 1 does not increase rapidly and the depletion capacitance of junction $J_2$is partially charged in a short period of time, I_{MOS} current is instantaneous. An expression for I_{MOS} can be obtained if we consider the collection-base junction depletion capacitance as in Fig. 3.1.

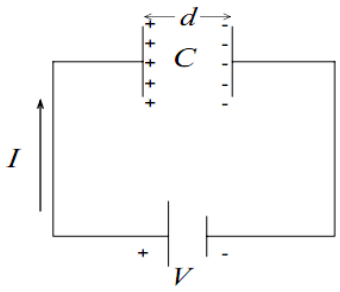

FIGURE 3.1: The collector-base depletion capacitance formation [14]

For the voltage V(t) between the plates, the charge per unit area q $=\frac{\in_{Si} V(t)}{d}$,where d is the distance between the plates and the rate of q change is ,

$$\frac{dq}{dt} = I(current)$$

As we know $q(t) = C_{bcj}(t)V(t)$, so

$$\frac{dq}{dt} = \frac{d}{dt}\left[C_{bcj}(t)V(t)\right]$$

$$= V(t)\frac{d_{bcj}(t)}{dt} + C_{bcj}(t)\frac{dV(t)}{dt}$$

and in terms of the junction capacitance of the reverse biased junction, the displacement current In(W(t)) is

$$I_n(W) = V(t)\frac{d_{bcj}(t)}{dt} + C_{bcj}(t)\frac{dV(t)}{dt} \qquad (3.1)$$

The first term on the right hand side of the equation (3.1) was ignored by Linear. The rate of change of $C_{bcj}(t)$ should be included in calculating the displacement current since the capacitance varies with time as the depletion width changes with voltage. From equation (2.6) and the fact that J = I/A, where A is the device active area,

$$I_n(W(t)) = \frac{I_T(t)}{1+\frac{1}{b}} + qAD\frac{\partial p(x,t)}{\partial x}$$

And from Linear's approach

$$I_n(W(t)) = C_{bcj}(t)\frac{dV(t)}{dt} = \frac{2qAD_p}{1+\frac{1}{b}}\frac{\partial p(x,t)}{\partial x}$$

$$\text{Or,}\left(1+\frac{1}{b}\right)C_{bcj}\frac{dV(t)}{dt} = I_T + 2qAD_p\frac{\partial p(x,t)}{\partial x} \qquad (3.2)$$

Linear used equation (3.2) to obtain V(t) for the transient operation of IGBT. He implemented the concept of moving the redistribution current. In his transient approach, he neither used the steady state expression for p(x) nor did he linearize the steady state expression for p(x). Moreover he assumed $C_{bcj}(t)$ to be constant with time, which is not so in reality.

His p(x) expression consists of two parts,

$$p(x) = P_0\left[1-\frac{x}{W(t)}\right] - \frac{P_0}{W(t)D}\left[\frac{x^2}{2} - \frac{W(t)x}{6} - \frac{x^3}{3W(t)}\right]\frac{dW(t)}{dt} \qquad (3.3)$$

From equation (2.6) & (3.3)

$$I_n(W(t)) = \frac{bI_T(t)}{1+b} + qAD\frac{\partial p(x)}{\partial x}$$

$$\text{Or, } I_n(W(t)) = \frac{I_T(t)}{1+\frac{1}{b}} + \frac{2qAD_P}{1+\frac{1}{b}}\frac{\partial p(x)}{\partial x} \qquad (3.4)$$

Instead of equation (3.1), Linear applied $I_n(W(t)) = C_{bcj}(t)\frac{dV}{dt}$ in his approach. Integrating

equation (3.3) in the base and multiplying by qA, the total charge Q,

$$Q = qA\int_0^W p(x)dx$$

$$= qA\left[x - \frac{x^2}{2W(t)}\right] - \frac{P_0}{W(t)D}\left[\frac{x^3}{6} - \frac{W(t)x^2}{12} - \frac{x^4}{12W(t)}\right]\frac{dW(t)}{dt}$$

$$= qA\left[P_0\left(W(t) - \frac{W(t)}{2}\right) - \frac{x^2}{2W(t)}\right] - \frac{P_0}{W(t)D}\left[\frac{x^3}{6} - \frac{W(t)x^2}{12} - \frac{x^4}{12W(t)}\right]\frac{dW(t)}{dt}$$

$$= \frac{qAP_0W(t)}{2} - \frac{qA}{P_0WD} \times 0$$

$$= \frac{qAP_0W(t)}{2} \qquad (3.5)$$

as can be seen $\frac{dW(t)}{dt}$ has no effect on Q calculation.

We can find $\frac{\partial p(x)}{\partial x}$ from equation (3.3) as when x=W(t)

$$\frac{\partial p(x)}{\partial x} = \frac{P_0}{W(t)} - \frac{P_0}{W(t)D}\left[\frac{2x}{2} - \frac{W(t)}{6} - \frac{3x^2}{W(t)}\right]\frac{dW(t)}{dt}$$

When *x=W(t)*

$$\frac{\partial p(x)}{\partial x} = \frac{-P_0}{W(t)} - \frac{P_0}{W(t)D}\left[W(t) - \frac{W(t)}{6} - W(t)\right]\frac{dW(t)}{dt}$$

$$\frac{\partial p(x)}{\partial x} = \frac{-P_0}{W(t)} - \frac{P_0}{6D}\frac{dW(t)}{dt}$$

The hole current is $-qA\frac{\partial p(x)}{\partial x}$ and from the above equation

$$-qAD\frac{\partial p(x)}{\partial x} = \frac{qADP_0}{W(t)} - \frac{qAP_0D}{6D}\frac{dW(t)}{dt}$$

As Q= $\frac{qAP_0W(t)}{2}$, from above equation

$$-qAD\frac{\partial p(x)}{\partial x} = \frac{2QD}{W^2(t)} - \frac{Q}{3W(t)}\frac{dW(t)}{dt} \qquad (3.6)$$

The first term on the right hand side of equation (3.6) is categorized by Linear asthe charge control component and the second term is categorized as the moving boundary redistribution component of the hole current.

From equation (3.4) and (3.6)

$$I_n(W(t)) = C\frac{dV(t)}{dt} = \frac{I_T(t)}{1+\frac{1}{b}} - \frac{4QD_P}{\left(1+\frac{1}{b}\right)W^2(t)} + \frac{Q}{3W(t)}\frac{dW(t)}{dt}$$

This equation can be expressed in a different way if in $-qA\frac{\partial P(x)}{\partial x}$ equation (3.6) is modified as

$$-qAD\frac{\partial p(x)}{\partial x} = \frac{-2qAD_p}{1+\frac{1}{b}}\frac{\partial p(x)}{\partial x}\frac{2QD}{W^2(t)} - \frac{Q}{3W(t)}\frac{dW(t)}{dt}$$

$$-2qAD_p\frac{\partial p(x)}{\partial x} = \frac{2QD}{W^2(t)}\left(1+\frac{1}{b}\right) - \frac{Q}{3W(t)}\left(1+\frac{1}{b}\right)\frac{dW(t)}{dt}$$

$$-2qAD_p\frac{\partial p(x)}{\partial x} = \frac{4D_pD_nQ}{W^2(t)(D_p+D_n)}\left(1+\frac{1}{b}\right) - \frac{Q}{3W(t)}\left(1+\frac{1}{b}\right)\frac{dW(t)}{dt}$$

$$-2qAD_p\frac{\partial p(x)}{\partial x} = \frac{4D_pQ}{W^2(t)} - \frac{Q}{3W(t)}\left(1+\frac{1}{b}\right)\frac{dW(t)}{dt} \qquad (3.7)$$

From equation (3.4), we have

$$I_n(W(t)) = C\frac{dV}{dt} = \frac{I_T(t)}{1+\frac{1}{b}} + \frac{2qAD_P}{1+\frac{1}{b}}\frac{\partial p(x)}{\partial x}$$

That can be rearranged as,

$$\left(1+\frac{1}{b}\right)C(t)\frac{dV}{dt} = I_T(t) + \frac{2qAD_P}{1+\frac{1}{b}}\frac{\partial p(x)}{\partial x}$$

Now using equation (3.7), and the fact that $C(t) = C_{bcj}(t) = \frac{A\varepsilon_{Si}}{W_{bcj}(t)} = A\sqrt{\frac{2\varepsilon_{Si}N_B}{2V(t)}}$ and $\frac{dW(t)}{dt} = \frac{-C}{qAN_B}\frac{dV(t)}{dt}$

the above equation yields

$$\left(1+\frac{1}{b}\right)C_{bcj}(t)\frac{dV(t)}{dt} = I_T(t) - \frac{4D_pQ}{W^2(t)} - \frac{Q}{3W(t)}\left(1+\frac{1}{b}\right)\frac{dW(t)}{dt}$$

$$\text{Or, } C_{bcj}(t)\frac{dV(t)}{dt}\left[1+\frac{Q}{3qAW(t)N_B}\right] = \frac{I_T(t) - \frac{4D_pQ}{W^2(t)}}{\left(1+\frac{1}{b}\right)}$$

$$\frac{dV(t)}{dt} = \frac{I_T(t) - \frac{4D_pQ}{W^2(t)}}{C_{bcj}(t)\left(1+\frac{1}{b}\right)\left[1+\frac{Q}{3qAW(t)N_B}\right]} \qquad (3.8)$$

Where $I_T(t)=I_T\ (0^-)$ for large inductive loads and $I_T(t) = \frac{4D_pQ(t)}{W^2(t)}$[Appendix A] forthe constant anode voltage in which$\frac{dV(t)}{dt} = 0$ indicating that the voltage W(t) are constants.

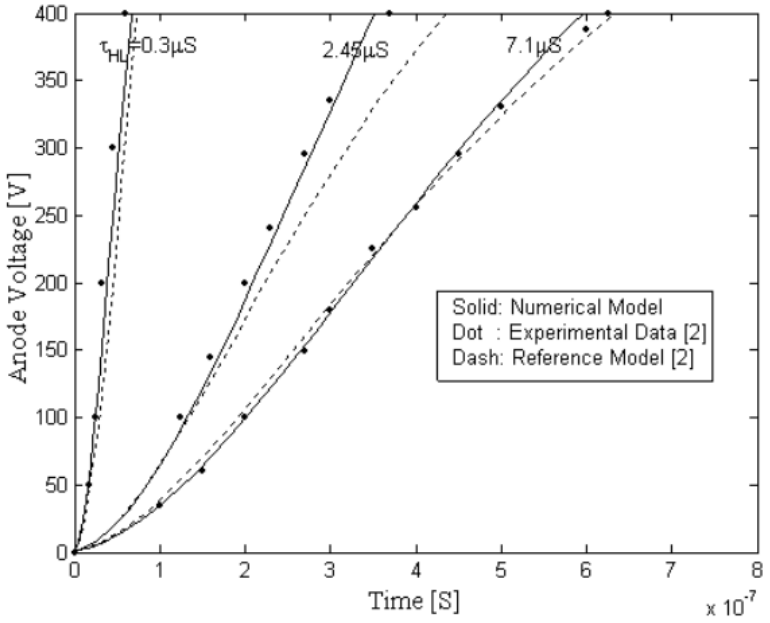

FIGURE 7.2: A comparison of the theoretical and measured 10A infinite inductive load switching voltage waveforms for devices with different base lifetimes [2]

Equation (3.8) is according to linear model transient $\frac{dV(t)}{dt}$ for IGBT and Q(t)is expressed by solving the following non-linear differential equation Parabolic by Linear

$$\frac{dQ(t)}{dt} = \frac{-Q(t)}{\tau_{HL}} - \frac{4Q^2(t)Isne}{W^2(t)A^2q^2n_i^2} \qquad (3.9)$$

Where I_{sne} is emitter electron saturation current (A) and n_i is the intrinsic carrier concentration (cm^{-3})

In the linear [2] approach, the negative of the collected hole current $I_p(W(t))$ consists of a charged control current (I_{cc}) and redistribution current (I_p), which make this model more

complex. The expression (3.9) is not simple and Q_0cannot be easily determined since there is no expression for P_0 which can be substituted for in Q_0 equation to evaluate Q_0 for magnitude. Also, this model did not considerthe rate of change of C(t) in the calculation of the displacement current I_n(W(t)).

3.1.2 Redistribution of time and Charge Control Current

Representative excess carrier distributions in the wide-base bipolar transient at various moments during a constant anode voltage turn-off transient are showing Fig. 3.3

When the base current is removed (constant anode voltage case) or the anode clamp voltage is reached (inductive load case), the carrier distribution in the base changes rapidly to one for which the total current at the emitter is equal to the hole current at the collector (from distribution (a) to (b) in Fig. 3.3), so that quasi-neutrality is maintained in the bipolar base. This reduction in the total device current is responsible for the initial rapid fall in current observed in the switching transient current waveform. The initial rapid fall consists principally of the steady-state net electron current at the collector (base current for the constant anode voltage case) and the component of hole drift current associated with the net electron current there. The remaining slowly decaying excess majority carrier store is responsible for the slowly decaying portion of the switching transient current wave form.

The boundary conditions on the electron and hole currents are different between the steady-state condition and the slowly decaying current phase. As a result, the electrons & holes that recombine can no longer be supplied be the divergence of their current densities as they are in steady-state, but are only supplied by (and thus reduce)the local excess carrier concentration. The curvature in the carrier distributions and the corresponding divergence of the current densities that remains after the initial rapid fall in emitter current acts to redistribute the excess carriers in the base from distribution (b) & (c) in Fig. 3.3.After the redistribution is complete, the excess carrier distribution and the terminal current are given in terms of the total excess carrier charge in the base, so the remainder of the waveform can be described using a charge control model. The redistribution time and the relation between the charge and current after the redistribution is complete are found from the time-dependent ambipolar diffusion equation with

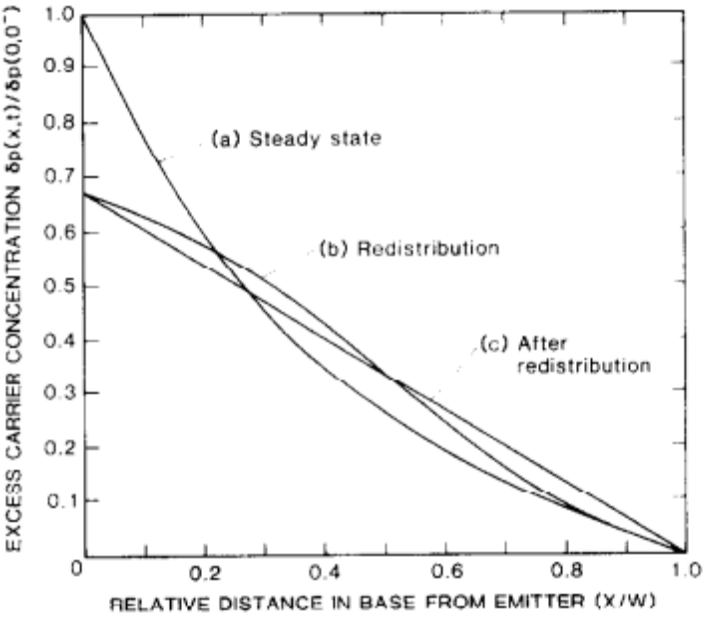

Figure 3.3: The Excess carrier distribution in the base before (a), during (b), and after (c) the redistribution phase of a constant anode voltage switching transient, for W/L=2.5 and for I_n(x= 0) <<I_p(x= 0). The effect of the decay of the total excess carrier has been left out to illustrate the redistribution process. [2]

I_n(W)=0 and the total current equal to emitter edge of the base for negligible electron current at the injected into the emitter to the collector current gives:

$$\frac{\partial P(x,t)}{\partial t} = \frac{\partial P(x,t)}{\partial t} \qquad (3.10)$$

The general solution to equation, $\frac{\partial^2 \delta p}{\partial x^2} = \frac{\partial p}{L^2} + \frac{1}{D}\frac{\partial \delta p}{\partial t}$

With the conditions of:

$$\delta p(x = 0, t = 0) = P_0 \qquad (3.11)$$

$$\delta p(W, t) = 0 \qquad (3.12)$$

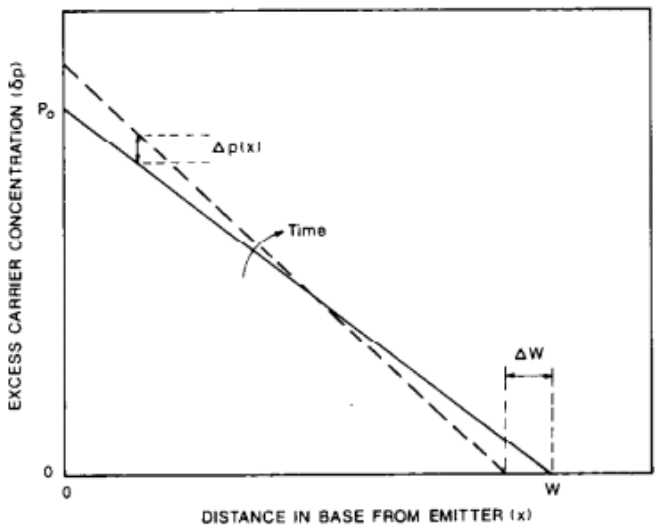

Figure 3.4: The carrier distribution in the base indicating the charge in excess carrier concentration with time due to the moving collector-base depletion edge boundary [2]

and equation (3.10) foe W independent of time is

$$\delta p(x,t) = P_{0,0}\left(1-\frac{x}{W}\right)e^{\left(\frac{-t}{\tau_{HL}}\right)} + \sum_{m=1}^{\infty} A_m \sin(2\pi mt)e^{\left(\frac{-t}{\tau m}\right)} \qquad (3.13)$$

Where

$$\frac{1}{\tau_m} = \frac{1}{\tau_{HL}} + \frac{(2m\pi)^2 D_p}{W^2} \qquad (3.14)$$

The first term of equation (3.13) is the linear charge control component of the distribution and the sine terms are the redistribution components which decay in timeτ_m. For the base width W_B= $93\times 10^{-6}m$ and other parameters, τ_m= $0.1/m^2us$.For times much larger than this, the redistribution terms become negligible and the current is determined by linear charge control component of the distribution.

The redistribution terms are independent of the total base charge and the integrated charge of the charge control term is equal to the total excess base charge:

$$Q(t) = \frac{qAP_{0,0}W}{2}e^{\left(-\frac{t}{\tau_{HL}}\right)} \qquad (3.16)$$

Therefore, the current can only be described by a charge control model after their distribution is complete. Using equations (3.13) & (3.15) for I_n(W) = 0, the chargecontrol current is [Appendix A]

$$I_T(t) = \frac{4D_p}{W^2} Q(t) \qquad (3.17)$$

Because the integrated charge of each of the redistribution terms is zero, the value of current obtained by extrapolating the current decay waveforms back to the time of the initial rapid fall in current corresponds to the value of current obtained from equation (3.16) evaluated for the initial charge.

In linear model it was assumed that the depletion capacitance ($C_{bcj}(t)$) to be constant throughout the whole process. But in reality, the depletion capacitance ($C_{bcj}(t)$) is a function of base depletion width (W_{bcj}(t)) as because

$$C_{bcj}(t) = \frac{A\varepsilon_{Si}}{W_{bcj}(t)}$$

The depletion capacitance is inversely proportional to the depletion width. So when the depletion width increases, capacitance decreases as well as effective base width (W(t)). This was not included in linear approach which is the main limitation of the model.

Chapter 4

Transient Analysis through Parabolic Approximation

The main foundation of the Parabolic model by Linear was based on the assumption that effective base width must be much less than the carrier diffusion length (W << L). But in case of base width greater than or equal to the diffusion length, the Parabolic models would give much variation than the experimental result. We have taken this limitation into account and have tried to propose a model that would give consistent result in all cases (W > L and W < L).

4.1 Approximation of Minority Carrier Concentration

In case of linear approximation, assuming,

$$W < L$$

So,

$$p(x,t) = P_0 \frac{\sin h\left(\frac{W-x}{L}\right)}{\sin h\left(\frac{W}{L}\right)}$$

turns to

$$p(x,t) = P_0 \left(1 - \frac{x}{L}\right) \quad (4.1)$$

But when

$$W > L$$

is assumed, the two curves show large deviation.

According to parabolic approximation,

$$\sin h\left(\frac{W-x}{L}\right) = \frac{W-x}{L} + \frac{1}{6}\left(\frac{W-x}{L}\right)^3$$

$$\sin h\left(\frac{W}{L}\right) = \frac{W}{L} + \frac{1}{6}\left(\frac{W}{L}\right)^3$$

For carrier concentration

$$p(x.t) = P_0 \frac{\frac{W(t)-x}{L} + \frac{1}{6}\left(\frac{W(t)-x}{L}\right)^3}{\frac{W(t)}{L} + \frac{1}{6}\left(\frac{W(t)}{L}\right)^3} \qquad (4.2)$$

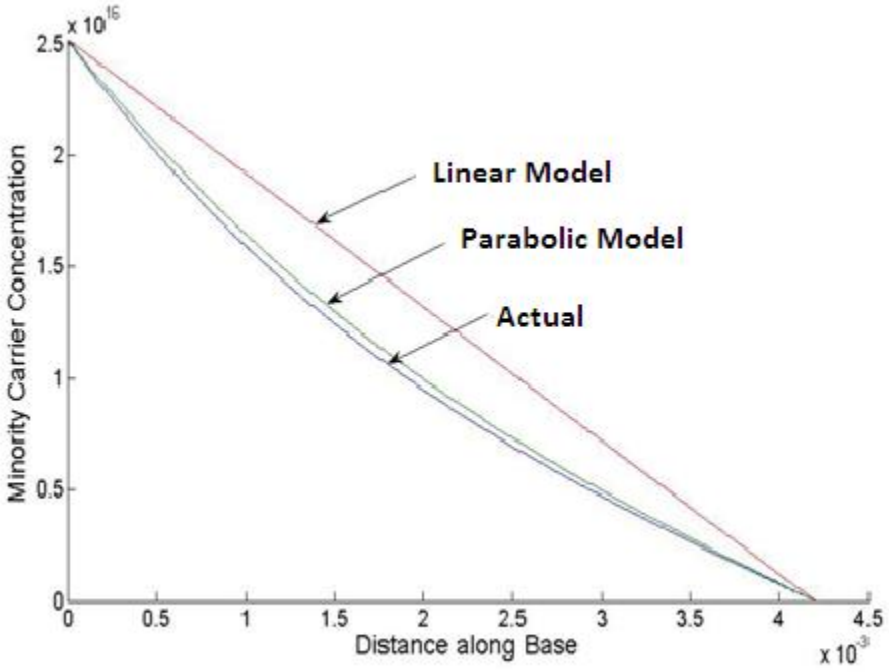

Figure 8.1: The carrier distribution in the base indicating the change in excess carrier concentration with distance in base for (W > L) (MATLAB)

which closely corresponds to the sinh curve for all values of W, unlike the linear approximation.

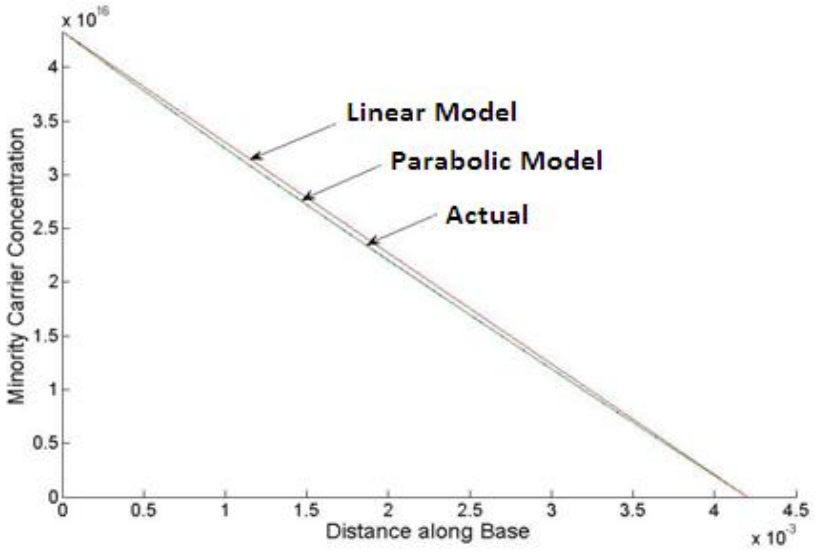

Figure 4.2: The carrier distribution in the base indicating the change in excess carrier concentration with distance in base for (W < L) (MATLAB).

$$p(x) = P_0 \frac{\frac{W-x}{L}+\frac{1}{6}\left(\frac{W-x}{L}\right)^3}{\frac{W}{L}+\frac{1}{6}\left(\frac{W}{L}\right)^3}$$

$$=P_0 \frac{\frac{6(W-x)L^2+(W-x)^3}{L^3}}{\frac{6WL^2+W^3}{L^3}}$$

$$=P_0 \frac{(W-x)\left[6L^2+(W-x)^2\right]}{W(6L^2+W^2)}$$

$$=P_0 \left(1-\frac{x}{W}\right)\frac{\left[6L^2+(W-x)^2\right]}{6L^2+W^2}$$

$$=P_0 \left[\frac{1+\frac{1}{6}\left(\frac{W-x}{L}\right)^2}{1+\frac{1}{6}\left(\frac{W}{L}\right)^2}\right]$$

So we have,

$$p(x,t) = P_0 \left[\frac{1+\frac{1}{6}(W(t)-x)^2}{1+\frac{1}{6}\left(\frac{W(t)}{L}\right)^2}\right] \qquad (4.3)$$

In linear approximation, the charge was found to be

$$Q_0 = qAP_o \frac{W}{2} \qquad (4.4)$$

and the actual value was

$$Q_0 = qAP_o L \tan h \left(\frac{W}{2L}\right) \qquad (4.5)$$

Taking the parabolic approximation,

$$\tan h \left(\frac{W}{2L}\right) = \frac{W}{2L} - \frac{1}{3}\left(\frac{W}{2L}\right)^3$$

So, we take steady state excess base charge as

$$Q_0 = qAP_o L \left[\frac{W}{2L} - \frac{1}{3}\left(\frac{W}{2L}\right)^3\right]$$

$$= qAP_o L \left[\frac{W}{2L} - \frac{W^3}{24L^3}\right]$$

$$= qAP_o \left[\frac{W}{2} - \frac{W^3}{24L^2}\right]$$

$$\text{So,} \quad P_0 = \frac{Q_0}{qA\left[\frac{W}{2} - \frac{W^3}{24L^2}\right]} \qquad (4.6)$$

Now,

$$\frac{\partial P_0}{\partial t} = \frac{Q_0}{qA}(-1)\left[\frac{1}{2}\frac{\partial W}{\partial t} - \frac{1}{24L^2}3W^2\frac{\partial W}{\partial t}\right]$$

$$= -\frac{P_0}{\left[\frac{W}{2} - \frac{W^3}{24L^2}\right]}\left[\frac{1}{2} - \frac{1}{8L^2}W^2\right]\frac{\partial W}{\partial t}$$

$$= -\frac{P_0}{W}\frac{24L^2}{(12L^2 - W^2)}\left[\frac{1}{2} - \frac{W^2}{8L^2}\right]\frac{\partial W}{\partial t} \qquad (4.7)$$

Now if we assume

$$W << L$$

$$\frac{\partial P_0}{\partial t} = -\frac{P_0}{W}\frac{24L^2}{12L^2}\frac{1}{2}\frac{\partial W}{\partial t}$$

$$\frac{\partial P_0}{\partial t} = -\frac{P_0}{W}\frac{\partial W}{\partial t} \qquad (4.8)$$

This is the deduced expression by Linear.

4.1.1 Ambipolar Diffusion Equations

$$\frac{\partial^2 p(x,t)}{\partial x^2} = \frac{p(x,t)}{L^2} + \frac{1}{D}\frac{\partial p(x,t)}{\partial t} \qquad (4.9)$$

Integrating once,

$$\frac{\partial p(x,t)}{\partial x} = \frac{1}{L^2}\int p(x,t)\partial x + \frac{1}{D}\int \frac{\partial p(x,t)}{\partial t}\partial x \qquad (4.10)$$

Again, integrating equation (4.10), we get

$$p(x,t) = -\frac{P_0}{4WL^2(6L^2+W^2)}\left[12L^2\frac{(W-x)^3}{-3} + \frac{(W-x)^5}{-5}\right]$$
$$+\frac{1}{D}\frac{P_0}{W}\frac{\partial W}{\partial t}\frac{1}{4W(6L^2+W^2)}\frac{(12L^2-3W^2)}{(12L^2-W^2)}\left[12L^2\frac{(W-x)^3}{-3} + \frac{(W-x)^5}{-5}\right]$$
$$+\frac{1}{D}P_0\frac{1}{W^2(6L^2+W^2)}\frac{\partial W}{\partial t}\left[\frac{x^3}{6}(6L^2+W^2) - 2W\frac{x^4}{12} + \frac{x^5}{20}\right]$$
$$+\frac{1}{D}\frac{2P_0}{W(6L^2+W^2)}\frac{\partial W}{\partial t}\left[W(W^2-6L^2)\frac{x^3}{6} - (2W^2-6L^2)\frac{x^4}{12} + W\frac{x^5}{20}\right] + C_1x + C_2 \qquad (4.11)$$

This is the expression for excess carrier concentration which is a function of x and t.

Boundary conditions:

$x = 0, p = p_0$ (4.12)

$x = W, p = 0$ (4.13)

Now putting the boundary values from equation (4.12) and (4.13) in equation (4.11), we get

$$p(x,t) = \frac{P_0}{4WL^2(6L^2+W^2)}\left[4L^2(W-x)^3 + \frac{(W-x)^5}{5}\right]$$
$$-\frac{1}{D}\frac{P_0}{W}\frac{\partial W}{\partial t}\frac{1}{4W(6L^2+W^2)}\frac{(12L^2-3W^2)}{(12L^2-W^2)}\left[4L^2(W-x)^3 + \frac{(W-x)^5}{5}\right]$$
$$+\frac{1}{D}P_0\frac{1}{W^2(6L^2+W^2)}\frac{\partial W}{\partial t}\left[\frac{x^3}{6}(6L^2+W^2) - W\frac{x^4}{6} + \frac{x^5}{20}\right]$$
$$+\frac{1}{D}\frac{2P_0}{W(6L^2+W^2)}\frac{\partial W}{\partial t}\left[W(W^2-6L^2)\frac{x^3}{6} - (2W^2-6L^2)\frac{x^4}{12} + W\frac{x^5}{20}\right]$$
$$-\frac{1}{D}\frac{P_0 x}{5}\frac{\partial W}{\partial t}\frac{(20L^2+W^2)}{(6L^2+W^2)}\left[\frac{(6L^2-W^2)}{(12L^2-W^2)}\right] - \frac{1}{D}\frac{P_0 x W^2}{(6L^2+W^2)^2}\frac{\partial W}{\partial t}\left[\frac{W^2-10L^2}{10}\right]$$
$$-\frac{p_0 x}{W} + \frac{P_0 x(20L^2+W^2)}{20(6L^2+W^2)}\frac{W}{L^2} + p_0 - \frac{P_0(20L^2+W^2)}{20(6L^2+W^2)}\left[\frac{W^2}{L^2} - \frac{1}{D}\frac{\partial W}{\partial t}\frac{(12L^2-3W^2)}{(12L^2-W^2)}.W\right] \qquad (4.13)$$

This is actual the excess carrier concentration $p(x,t)$for base n-drift region.

Now we know, the excess base charge can be calculated by the following equation

$$Q(t) = qA\int_0^W p(x)dx \qquad (4.14)$$

Integrating the excess carrier concentration, we get

$$\int p(x,t)dx = \frac{P_0}{20WL^2(6L^2+W^2)}\left[\frac{20L^2(W-x)^4}{-4} - \frac{(W-x)^6}{6}\right]$$
$$-\frac{1}{D}\frac{P_0}{20W^2}\frac{\partial W}{\partial t}\frac{1}{(6L^2+W^2)}\frac{(12L^2-3W^2)}{(12L^2-W^2)}\left[\frac{20L^2(W-x)^4}{-4} - \frac{(W-x)^6}{6}\right]$$
$$+\frac{1}{D}P_0\frac{1}{W^2(6L^2+W^2)}\frac{\partial W}{\partial t}\left[\frac{x^4}{24}(6L^2+W^2) - W\frac{x^5}{30} + \frac{x^6}{120}\right]$$
$$+\frac{1}{D}\frac{2P_0}{W(6L^2+W^2)}\frac{\partial W}{\partial t}\left[W(W^2-6L^2)\frac{x^4}{24} - (W^2-3L^2)\frac{x^5}{30} + W\frac{x^6}{120}\right]$$
$$-\frac{1}{D}\frac{P_0}{5}\frac{\partial W}{\partial t}\frac{(20L^2+W^2)}{(6L^2+W^2)}\left[\frac{(6L^2-W^2)}{(12L^2-W^2)}\right]\frac{x^2}{2}$$
$$-\frac{1}{D}\frac{P_0 W^2}{(6L^2+W^2)^2}\frac{\partial W}{\partial t}\left[\frac{W^2-10L^2}{10}\right]\frac{x^2}{2}$$

$$-\frac{p_0}{W}\frac{x^2}{2}+\frac{P_0(20L^2+W^2)}{20(6L^2+W^2)}\frac{W}{L^2}\frac{x^2}{2}+p_0x-\frac{P_0(20L^2+W^2)}{20(6L^2+W^2)}\left[\frac{W^2}{L^2}-\frac{1}{D}\frac{\partial W}{\partial t}\frac{(12L^2-3W^2)}{(12L^2-W^2)}.W\right]x \qquad (4.15)$$

Now we putting $x = W$ (upper limit) and $x = 0$ (lower limit) in $\int p(x,t)dx$ and if we assume W is much much smaller than L (W << L)

$$\int_0^W Pdx = \frac{1}{D}\frac{P_0W^2}{24}\frac{\partial W}{\partial t}$$

$$-\frac{1}{D}\frac{P_0W^4}{120L^2}\frac{\partial W}{\partial t}-\frac{1}{D}\frac{P_0W^2}{6}\frac{\partial W}{\partial t}+\frac{1}{D}\frac{P_0W^4}{72L^2}\frac{\partial W}{\partial t}+P_0\frac{W}{2}+\frac{P_0W^3}{12L^2}$$

$$-\frac{P_0W^3}{6L^2}+\frac{1}{D}\frac{P_0W^2}{6L^2}\frac{\partial W}{\partial t}+\frac{P_0W^3}{24L^2}-\frac{1}{D}\frac{P_0W^2}{4}\frac{\partial W}{\partial t}$$

$$\int_0^W Pdx = P_0\frac{W}{2}-\frac{P_0W^3}{24L^2}-\frac{3}{8}\frac{1}{D}P_0W^2\frac{\partial W}{\partial t} \qquad (4.16)$$

Now the excess base charge will be

$$Q(t) = qA\int_0^W Pdx$$

$$= qAP_0\frac{W}{2}-qA\frac{P_0W^3}{24L^2}-qA\frac{3P_0W^2}{8D}\frac{\partial W}{\partial t}$$

$$= qA\left[P_0\frac{W}{2}-\frac{P_0W^3}{24L^2}\right]-qA\frac{3P_0W^2}{8D}\frac{\partial W}{\partial t} \qquad (4.17)$$

As we know,

$$\text{L}=\sqrt{D\tau_{HL}}$$

So, $L^2 = D\tau_{HL}$, $\tau_{HL} = 5\times10^{-7}(\frac{T}{300})^{1.5}$

So, $D = \frac{L^2}{\tau_{HL}}$

$$qA\frac{3P_0W^2}{8D}\frac{\partial W}{\partial t} = qA\frac{3}{8}\frac{L^2}{W^2}P_0\frac{\partial W}{\partial t}\tau_{HL} \approx 0$$

As, $\frac{W}{L} << 1$

$$Q(t) = qA\left[P_0\frac{W}{2} - \frac{P_0W^3}{24L^2}\right] \quad (4.18)$$

Assuming $\frac{W}{L} << 1, \frac{W^3}{L^2} \approx 0$

$$Q(t) = qA\frac{P_0W(t)}{2} \quad (4.19)$$

4.2 Expression for Transient Anode Voltage

According to Allen R.Linear:

$$p(x,t) = P_0\left[1 - \frac{x}{W(t)}\right] - \frac{1}{W(t)}\frac{\partial W}{\partial t}\frac{P_0}{D}\left[\frac{x^2}{2} - \frac{W(t)x}{6} - \frac{x^3}{3W(t)}\right] \quad (4.20)$$

In Parabolic model,

$$p(x,t) = \frac{P_0}{4WL^2(6L^2+W^2)}\left[4L^2(W-x)^3 + \frac{(W-x)^5}{5}\right]$$
$$-\frac{1}{D}\frac{P_0}{W}\frac{\partial W}{\partial t}\frac{1}{4W(6L^2+W^2)}\frac{(12L^2-3W^2)}{(12L^2-W^2)}\left[4L^2(W-x)^3 + \frac{(W-x)^5}{5}\right]$$
$$+\frac{1}{D}P_0\frac{1}{W^2(6L^2+W^2)}\frac{\partial W}{\partial t}\left[\frac{x^3}{6}(6L^2+W^2) - W\frac{x^4}{6} + \frac{x^5}{20}\right]$$
$$+\frac{1}{D}\frac{2P_0}{W(6L^2+W^2)^2}\frac{\partial W}{\partial t}\left[W(W^2-6L^2)\frac{x^3}{6} - (2W^2-6L^2)\frac{x^4}{12} + W\frac{x^5}{20}\right]$$
$$-\frac{1}{D}\frac{P_0x}{5}\frac{\partial W}{\partial t}\frac{(20L^2+W^2)}{(6L^2+W^2)}\left[\frac{(6L^2-W^2)}{(12L^2-W^2)}\right] - \frac{1}{D}\frac{P_0xW^2}{(6L^2+W^2)^2}\frac{\partial W}{\partial t}\left[\frac{W^2-10L^2}{10}\right]$$
$$-\frac{p_0x}{W} + \frac{P_0x(20L^2+W^2)}{20(6L^2+W^2)}\frac{W}{L^2} + p_0 - \frac{P_0(20L^2+W^2)}{20(6L^2+W^2)}\left[\frac{W^2}{L^2} - \frac{1}{D}\frac{\partial W}{\partial t}\frac{(12L^2-3W^2)}{(12L^2-W^2)}.W\right] \quad (4.21)$$

$I_n(W) =$ Displacement current

It is created from discharge of Reverse Biased Collector Base Depletion Junction

Capacitance $C_{bcj}(t)$

In his journal, Linear assumed $C_{bcj}(t)$ to be constant all through time which is not correct. $C_{bcj}(t)$ Varies with depletion width $W_{bcj}(t)$, which is a function of time.

$$I_n(W) = \frac{d}{dt}\left(C_{bcj}V_{CE}\right)$$

$$I_n(W) = V_{CE}\frac{dC_{bcj}}{dt} + C_{bcj}\frac{dV_{CE}}{dt}$$

Now,

$$C_{bcj} = \frac{A \in_{si}}{W_{bcj}}$$

Here,

$$W_{bcj} = \sqrt{\frac{\in_{Si} V_{CE}}{qN_B}}$$

So,

$$C_{bcj} = A \in_{si} \sqrt{\frac{qN_B}{2\in_{si} V_{CE}}}$$

As we know

$$W = W_B - W_{bcj}$$

$$\frac{dW}{dt} = -\frac{dC_{bcj}}{dt} \qquad (4.22)$$

where,

W_B =Total Base Width

W = Effective Base Width

W_{bcj}= Depletion Region Width

So we get

$$\frac{dW_{bcj}}{dt} = \frac{1}{2}\sqrt{\frac{qN_B}{2 \in_{si} V_{CE}}}\frac{2 \in_{si}}{qN_B}\frac{dV_{CE}}{dt}$$

$$= \sqrt{\frac{q \in_{si} N_B}{2V_{CE}}}\frac{1}{qN_B}\frac{dV_{CE}}{dt}$$

$$=\frac{C_{bcj}}{qAN_B}\frac{dV_{CE}}{dt}$$

$$\frac{dW}{dt} = -\frac{C_{bcj}}{qAN_B}\frac{dV_{CE}}{dt} \qquad (4.23)$$

$$\frac{dC_{bcj}}{dt} = A\frac{d}{dt}\sqrt{\frac{q \in_{si} N_B}{2V_{CE}}}$$

$$= -A\frac{1}{2}\frac{1}{\sqrt{\frac{q \in_{si} N_B}{2V_{CE}}}}\frac{q \in_{si} N_B}{2}\frac{1}{{V_{CE}}^2}\frac{dV_{CE}}{dt}$$

$$= -\frac{1}{2}\frac{A^2}{C_{bcj}}\frac{q \in_{si} N_B}{2}\frac{1}{{V_{CE}}^2}\frac{dV_{CE}}{dt}$$

$$V_{CE}\frac{dC_{bcj}}{dt} = -\frac{1}{4}\frac{A^2}{C_{bcj}}\frac{q \in_{si} N_B}{V_{CE}}\frac{dV_{CE}}{dt}$$

So the displacement current is

$$I_n(W) = -\frac{1}{4}\frac{A^2}{C_{bcj}}\frac{q \in_{si} N_B}{V_{CE}}\frac{dV_{CE}}{dt} + C_{bcj}\frac{dV_{CE}}{dt}$$

$$=C_{bcj}\frac{dV_{CE}}{dt}\left[-\frac{1}{4}\frac{A^2}{{C_{bcj}}^2}\frac{q \in_{si} N_B}{V_{CE}} + 1\right]$$

$$= C_{bcj}\frac{dV_{CE}}{dt}\left[-\frac{1}{4}\frac{2V_{CE}}{q \in_{si} N_B}\frac{q \in_{si} N_B}{V_{CE}} + 1\right]$$

$$= C_{bcj}\frac{dV_{CE}}{dt}\left[1-\frac{1}{2}\right]$$

$$= \frac{1}{2}C_{bcj}\frac{dV_{CE}}{dt} \qquad (4.24)$$

Now, Displacement Current Equation with Transistor Current & Diffusion Current

$$I_n(W) = \frac{I_T}{1+\frac{1}{b}} + qAD\frac{\partial p(x,t)}{\partial x}_{[x=W(t)]}$$

Now,

From Our equation of $p(x,t)$,we get

$$\frac{\partial p(x,t)}{\partial t} = \frac{P_0}{20WL^2(6L^2+W^2)}[20L^2 3(W-x)^2(-1)+5(W-x)^4(-1)]$$

$$-\frac{1}{D}\frac{P_0}{20W^2}\frac{\partial W}{\partial t}\frac{1}{(6L^2+W^2)}\frac{(12L^2-3W^2)}{(12L^2-W^2)}[20L^2 3(W-x)^2(-1)+5(W-x)^4(-1)]$$

$$+\frac{1}{D}P_0\frac{1}{W^2(6L^2+W^2)}\frac{\partial W}{\partial t}\left[\frac{3x^2}{6}(6L^2+W^2)-W\frac{4x^3}{6}+\frac{5x^4}{20}\right]$$

$$+\frac{1}{D}\frac{2P_0}{W(6L^2+W^2)^2}\frac{\partial W}{\partial t}\left[W(W^2-6L^2)\frac{3x^2}{6}-(W^2-3L^2)\frac{4x^3}{6}+W\frac{5x^4}{20}\right]$$

$$-\frac{1}{D}\frac{P_0}{5}\frac{\partial W}{\partial t}\frac{(20L^2+W^2)}{(6L^2+W^2)}\left[\frac{(6L^2-W^2)}{(12L^2-W^2)}\right]$$

$$-\frac{1}{D}\frac{P_0W^2}{(6L^2+W^2)^2}\frac{\partial W}{\partial t}\left[\frac{W^2-10L^2}{10}\right]$$

$$-\frac{p_0}{W}+\frac{P_0(20L^2+W^2)}{20(6L^2+W^2)}\frac{W}{L^2}$$

$$\frac{\partial p(x,t)}{\partial t} = \frac{P_0}{20WL^2(6L^2+W^2)}[20L^2 3(W-x)^2(-1)+5(W-x)^4(-1)]$$

$$-\frac{1}{D}\frac{P_0}{20W^2}\frac{\partial W}{\partial t}\frac{1}{(6L^2+W^2)}\frac{(12L^2-3W^2)}{(12L^2-W^2)}[20L^2 3(W-x)^2(-1)+5(W-x)^4(-1)]$$

$$+\frac{1}{D}P_0\frac{1}{W^2(6L^2+W^2)}\frac{\partial W}{\partial t}\left[\frac{3x^2}{6}(6L^2+W^2)-W\frac{4x^3}{6}+\frac{5x^4}{20}\right]$$

$$+\frac{1}{D}\frac{2P_0}{W(6L^2+W^2)^2}\frac{\partial W}{\partial t}\left[W(W^2-6L^2)\frac{3x^2}{6}-(W^2-3L^2)\frac{4x^3}{6}+W\frac{5x^4}{20}\right]$$

$$-\frac{1}{D}\frac{P_0}{5}\frac{\partial W}{\partial t}\frac{(20L^2+W^2)}{(6L^2+W^2)}\left[\frac{(6L^2-W^2)}{(12L^2-W^2)}\right]$$

$$-\frac{1}{D}\frac{P_0W^2}{(6L^2+W^2)^2}\frac{\partial W}{\partial t}\left[\frac{W^2-10L^2}{10}\right]$$

$$-\frac{p_0}{W}+\frac{P_0(20L^2+W^2)}{20(6L^2+W^2)}\frac{W}{L^2}$$

$$\frac{\partial p(x,t)}{\partial t}_{x=W}=\frac{1}{D}\frac{P_0}{W^2(6L^2+W^2)}\frac{\partial W}{\partial t}\left[\frac{W^2}{2}(6L^2+W^2)-\frac{2W^4}{3}+\frac{W^4}{4}\right]$$

$$+\frac{1}{D}\frac{2P_0}{W(6L^2+W^2)^2}\frac{\partial W}{\partial t}\left[W(W^2-6L^2)\frac{w^2}{2}-(W^2-3L^2)\frac{2w^3}{3}+\frac{w^5}{4}\right]$$

$$-\frac{1}{D}\frac{P_0}{5}\frac{\partial W}{\partial t}\frac{(20L^2+W^2)}{(6L^2+W^2)}\left[\frac{(6L^2-W^2)}{(12L^2-W^2)}\right]$$

$$-\frac{1}{D}\frac{P_0W^2}{(6L^2+W^2)^2}\frac{\partial W}{\partial t}\left[\frac{W^2-10L^2}{10}\right]$$

$$-\frac{p_0}{W}+\frac{P_0(20L^2+W^2)}{20(6L^2+W^2)}\frac{W}{L^2}$$

$$\frac{\partial p(x,t)}{\partial t}_{x=W}=\frac{1}{D}\frac{P_0}{(6L^2+W^2)}\frac{\partial W}{\partial t}\left[3L^2+\frac{W^2}{2}-\frac{5W^2}{12}\right]$$

$$+\frac{1}{D}\frac{P_0}{(6L^2+W^2)^2}\frac{\partial W}{\partial t}\left[W^4-6L^2W^2-\frac{4}{3}(W^2-3L^2)W^2+\frac{W^4}{2}\right]$$

$$-\frac{1}{D}\frac{P_0}{5}\frac{\partial W}{\partial t}\frac{(20L^2+W^2)}{(6L^2+W^2)}\left[\frac{(6L^2-W^2)}{(12L^2-W^2)}\right]-\frac{1}{D}\frac{P_0}{(6L^2+W^2)^2}\frac{\partial W}{\partial t}\left[\frac{W^4-10L^2W^2}{10}\right]$$

$$-\frac{p_0}{W}+\frac{P_0(20L^2+W^2)}{20(6L^2+W^2)}\frac{W}{L^2}$$

$$\frac{\partial p(x,t)}{\partial t}_{x=W}=\frac{1}{D}\frac{P_0}{(6L^2+W^2)}\frac{\partial W}{\partial t}\left[3L^2+\frac{W^2}{12}\right]$$

$$+\frac{1}{D}\frac{P_0}{(6L^2+W^2)^2}\frac{\partial W}{\partial t}\left[W^4-6L^2W^2-\frac{4}{3}W^4+4L^2W^2+\frac{W^4}{2}\right]$$

$$-\frac{1}{D}\frac{P_0}{5}\frac{\partial W}{\partial t}\frac{(20L^2+W^2)}{(6L^2+W^2)}\left[\frac{(6L^2-W^2)}{(12L^2-W^2)}\right]-\frac{1}{D}\frac{P_0}{(6L^2+W^2)^2}\frac{\partial W}{\partial t}\left[\frac{W^4-10L^2W^2}{10}\right]$$
$$-\frac{p_0}{W}+\frac{P_0(20L^2+W^2)}{20(6L^2+W^2)}\frac{W}{L^2}$$

$$\frac{\partial p(x,t)}{\partial t}_{x=W}=\frac{1}{D}\frac{P_0}{(6L^2+W^2)}\frac{\partial W}{\partial t}\left[3L^2+\frac{W^2}{12}\right]+\frac{1}{D}\frac{P_0}{(6L^2+W^2)^2}\frac{\partial W}{\partial t}\left[\frac{1}{6}W^4-2L^2W^2\right]$$
$$-\frac{1}{D}\frac{P_0}{5}\frac{\partial W}{\partial t}\frac{(20L^2+W^2)}{(6L^2+W^2)}\left[\frac{(6L^2-W^2)}{(12L^2-W^2)}\right]-\frac{1}{D}\frac{P_0}{(6L^2+W^2)^2}\frac{\partial W}{\partial t}\left[\frac{W^4-10L^2W^2}{10}\right]$$
$$-\frac{p_0}{W}+\frac{P_0(20L^2+W^2)}{20(6L^2+W^2)}\frac{W}{L^2}$$

We know from parabolic approximation, the excess carrier concentration at $x=0$ would be

$$P_0=\frac{Q}{qA\left[\frac{W}{2}-\frac{W^3}{24L^2}\right]}$$

So,

$$qAD\frac{\partial p(x,t)}{\partial t}_{x=W}=qA\frac{P_0}{(6L^2+W^2)}\frac{\partial W}{\partial t}\left[3L^2+\frac{W^2}{12}\right]+qA\frac{P_0}{(6L^2+W^2)^2}\frac{\partial W}{\partial t}\left[\frac{1}{6}W^4-2L^2W^2\right]$$
$$-\text{qA}\frac{P_0}{5}\frac{\partial W}{\partial t}\frac{(20L^2+W^2)}{(6L^2+W^2)}\left[\frac{(6L^2-W^2)}{(12L^2-W^2)}\right]-qA\frac{P_0}{(6L^2+W^2)^2}\frac{\partial W}{\partial t}\left[\frac{W^4-10L^2W^2}{10}\right]$$
$$-qADp_0\left[\frac{1}{W}-\frac{1}{20}\frac{W}{L^2}\frac{(20L^2+W^2)}{(6L^2+W^2)}\right]$$

$$qAD\frac{\partial p(x,t)}{\partial t}_{x=W} = qA\frac{Q}{qA\left[\frac{W}{2}-\frac{W^3}{24L^2}\right]}\left(-\frac{C_{bcj}}{qAN_B}\frac{dV_{CE}}{dt}\right)\left[\frac{3L^2+\frac{W^2}{12}}{(6L^2+W^2)}\right]$$

$$+qA\frac{Q}{qA\left[\frac{W}{2}-\frac{W^3}{24L^2}\right]}\left(-\frac{C_{bcj}}{qAN_B}\frac{dV_{CE}}{dt}\right)\left[\frac{\frac{1}{6}W^4-2L^2W^2}{(6L^2+W^2)^2}\right]$$

$$-\text{qA}\frac{Q}{qA\left[\frac{W}{2}-\frac{W^3}{24L^2}\right]}\left(-\frac{C_{bcj}}{qAN_B}\frac{dV_{CE}}{dt}\right)\frac{(20L^2+W^2)}{(6L^2+W^2)}\left[\frac{(6L^2-W^2)}{(12L^2-W^2)}\right]$$

$$-qA\frac{Q}{qA\left[\frac{W}{2}-\frac{W^3}{24L^2}\right]}\left(-\frac{C_{bcj}}{qAN_B}\frac{dV_{CE}}{dt}\right)\frac{1}{(6L^2+W^2)^2}\left[\frac{W^4-10L^2W^2}{10}\right]$$

$$-qAD\frac{Q}{qA\left[\frac{W}{2}-\frac{W^3}{24L^2}\right]}\left[\frac{1}{W}-\frac{1}{20}\frac{W}{L^2}\frac{(20L^2+W^2)}{(6L^2+W^2)}\right]$$

$$qAD\frac{\partial p(x,t)}{\partial t}_{x=W} = \frac{Q}{\left[\frac{W}{2}-\frac{W^3}{24L^2}\right]}\left(-\frac{C_{bcj}}{qAN_B}\frac{dV_{CE}}{dt}\right)\left[\frac{3L^2+\frac{W^2}{12}}{(6L^2+W^2)}-\frac{1}{5}\frac{(20L^2+W^2)}{(6L^2+W^2)}\frac{(6L^2-W^2)}{(12L^2-W^2)}\right]$$

$$-\frac{Q}{\left[\frac{W}{2}-\frac{W^3}{24L^2}\right]}\left(-\frac{C_{bcj}}{qAN_B}\frac{dV_{CE}}{dt}\right)\frac{1}{(6L^2+W^2)^2}\left[\frac{1}{6}W^4-2L^2W^2\frac{W^4-10L^2W^2}{10}\right]$$

$$-D\frac{Q}{\left[\frac{W}{2}-\frac{W^3}{24L^2}\right]}\left[\frac{1}{W}-\frac{1}{20}\frac{W}{L^2}\frac{(20L^2+W^2)}{(6L^2+W^2)}\right]$$

As we know, the displacement current

$$I_n(W) = \frac{I_T}{1+\frac{1}{b}} + qAD\frac{\partial p(x,t)}{\partial x}_{[x=W(t)]}$$

$$\frac{1}{2}C_{bcj}\frac{dV_{CE}}{dt} = \frac{I_T}{1+\frac{1}{b}} + \frac{Q}{\left[\frac{W}{2}-\frac{W^3}{24L^2}\right]}\left(-\frac{C_{bcj}}{qAN_B}\frac{dV_{CE}}{dt}\right)$$

$$\left[\frac{3L^2+\frac{W^2}{12}}{(6L^2+W^2)}-\frac{1}{5}\frac{(20L^2+W^2)}{(6L^2+W^2)}\frac{(6L^2-W^2)}{(12L^2-W^2)}+\frac{\frac{1}{6}W^4-2L^2W^2}{(6L^2+W^2)^2}-\frac{W^4-10L^2W^2}{10}\right]$$

$$-D\frac{Q}{\left[\frac{W}{2}-\frac{W^3}{24L^2}\right]}\left[\frac{1}{W}-\frac{1}{20}\frac{W}{L^2}\frac{(20L^2+W^2)}{(6L^2+W^2)}\right]$$

$$\frac{1}{2}C_{bcj}\frac{dV_{CE}}{dt}\left[1+\frac{2Q}{qAN_B\left[\frac{W}{2}-\frac{W^3}{24L^2}\right]}\left(\frac{3L^2+\frac{W^2}{12}}{(6L^2+W^2)}-\frac{1}{5}\frac{(20L^2+W^2)}{(6L^2+W^2)}\frac{(6L^2-W^2)}{(12L^2-W^2)}+\frac{\frac{1}{15}W^4-L^2W^2}{(6L^2+W^2)^2}\right)\right]$$

$$=\frac{1}{1+\frac{1}{b}}\left[I_T(0)-D\frac{Q\left(1+\frac{1}{b}\right)}{\left[\frac{W}{2}-\frac{W^3}{24L^2}\right]}\left[\frac{1}{W}-\frac{1}{20}\frac{W}{L^2}\frac{(20L^2+W^2)}{(6L^2+W^2)}\right]\right]$$

$$\frac{dV_{CE}}{dt}=\frac{I_T(t)-\frac{2D_PQ(t)}{\left[\frac{W}{2}-\frac{W^3}{24L^2}\right]}\left[\frac{1}{W}-\frac{1}{20L^2}\frac{W(20L^2+W^2)}{(6L^2+W^2)}\right]}{\frac{1}{2}C_{bcj}\left(1+\frac{1}{b}\right)\left[1+\frac{2Q(t)}{qAN_B\left[\frac{W}{2}-\frac{W^3}{24L^2}\right]}\left(\frac{3L^2+\frac{W^2}{12}}{(6L^2+W^2)}-\frac{1(20L^2+W^2)(6L^2-W^2)}{5(6L^2+W^2)(12L^2-W^2)}+\frac{\frac{1}{15}W^4-L^2W^2}{(6L^2+W^2)^2}\right)\right]} \quad (4.25)$$

This is the analytical expression for transient voltage of Non Punch IGBT.

Now if we assume,

$$W << L$$

$$\frac{W}{L} << 1$$

Then,

$$20L^2+W^2=20L^2$$

$$6L^2+W^2=6L^2$$

$$3L^2+\frac{W^2}{12}=3L^2$$

Now, $$\frac{dV_{CE}}{dt}=\frac{I_T(t)-\frac{2D_PQ(t)}{\left[\frac{W}{2}-\frac{W^3}{24L^2}\right]}\left[\frac{1}{W}-\frac{1}{20L^2}\frac{W(20L^2+W^2)}{(6L^2+W^2)}\right]}{\frac{1}{2}C_{bcj}\left(1+\frac{1}{b}\right)\left[1+\frac{2Q(t)}{qAN_B\left[\frac{W}{2}-\frac{W^3}{24L^2}\right]}\left(\frac{3L^2+\frac{W^2}{12}}{(6L^2+W^2)}-\frac{1(20L^2+W^2)(6L^2-W^2)}{5(6L^2+W^2)(12L^2-W^2)}+\frac{\frac{1}{15}W^4-L^2W^2}{(6L^2+W^2)^2}\right)\right]}$$

$$=\frac{I_T(t)-\frac{2D_PQ(t)}{\left[\frac{W}{2}\right]}\left[\frac{1}{W}-\frac{1}{20L^2}\frac{W(20L^2)}{(6L^2)}\right]}{\frac{1}{2}C_{bcj}\left(1+\frac{1}{b}\right)\left[1+\frac{2Q(t)}{qAN_B\left[\frac{W}{2}\right]}\left(\frac{3L^2}{6L^2}-\frac{1(20L^2)(6L^2)}{5(6L^2)(12L^2)}+\frac{\frac{1}{15}W^4-L^2W^2}{36L^4}\right)\right]}$$

$$= \frac{I_T(t) - 4D_P\left[\frac{1}{W^2} - \frac{1}{6L^2}\right]Q(t)}{\frac{1}{2}C_{bcj}\left(1+\frac{1}{b}\right)\left[1+\frac{4Q(t)}{qAN_BW}\frac{1}{6}\right]}$$

$$\frac{dV_{CE}}{dt} = \frac{I_T(t) - 4D_P\left[\frac{1}{W^2} - \frac{1}{6L^2}\right]Q(t)}{\frac{1}{2}C_{bcj}\left(1+\frac{1}{b}\right)\left[1+\frac{2Q(t)}{3qAN_BW}\right]} \qquad (4.26)$$

Assuming,

$$W << L$$

$$\frac{1}{W^2} >> \frac{1}{6L^2}$$

So we neglect $\frac{1}{6L^2}$ terms find out

$$\frac{dV_{CE}}{dt} = \frac{I_T(t) - \frac{4D_PQ(t)}{W(t)^2}}{\frac{1}{2}C_{bcj}\left(1+\frac{1}{b}\right)\left[1+\frac{2Q(t)}{3qAN_BW}\right]} \qquad (4.27)$$

This is the expression for the transient voltage derived by Allen R. Linear Jr & David L. Blackburn (1988) in the journal [2].

4.3 Expression for stored charge decay:

Here, due to the injection into the emitter, stored charge in the base would decay. The total charge decay rate would be

$$\frac{dQ(t)}{dt} = -\frac{Q(t)}{\tau_{HL}} - I_n(0)$$

Using the quasi-equilibrium simplification (i,e. the difference between the electron & hole quasi fermi potentials is the same on the both sides of the junction) and assuming high-level injection of the holes into the base, the electron current at the emitter-base junction $I_n(0)$ is related to $P_n(0)$ by :

$$\frac{I_n(0)}{I_{sne}} = e^{\frac{q}{kt}(\varphi_{pej} - \varphi_{nej})} = \frac{P_0(N_B + P_0)}{n_i^2} \approx \frac{P_0^2}{n_i^2}$$

Where,

φ_{nej}=Electron quasi fermi potential at E-B junction.

φ_{pej}=Hole quasi fermi potential at E-B junction.

I_{sne}=Emitter electron saturation current which accounts or the emitter parameters (Similar to the emitter Gummel Number).

The approximate form follows from the assumption that the basic is in high-level injection. Now we presume

$$P_0 = \frac{Q}{qA\left[\frac{W}{2} - \frac{W^3}{24L^2}\right]}$$

$$I_n(0) = \frac{P_0^2}{n_i^2} I_{sne}$$

$$I_n(0) = \frac{Q^2}{q^2A^2\left[\frac{W}{2} - \frac{W^3}{24L^2}\right]^2} \frac{I_{sne}}{n_i^2}$$

$$\frac{dQ(t)}{dt} = -\frac{Q(t)}{\tau_{HL}} - \frac{Q^2}{q^2A^2\left[\frac{W}{2} - \frac{W^3}{24L^2}\right]^2} \frac{I_{sne}}{n_i^2} \qquad (4.28)$$

This is the expression for the stored charge decay rate

If

$$W << L$$

Then

$$\frac{W^3}{24L^2} \approx 0$$

So,

$$\frac{dQ(t)}{dt} \approx -\frac{Q(t)}{\tau_{HL}} - \frac{Q(t)^2}{q^2A^2\frac{W(t)^2}{4}} \frac{I_{sne}}{n_i^2}$$

$$\approx -\frac{Q(t)}{\tau_{HL}} - \frac{4Q(t)^2}{q^2A^2W(t)^2} \frac{I_{sne}}{n_i^2}$$

$$\frac{dQ(t)}{dt} \approx -\frac{Q(t)}{\tau_{HL}} - \frac{4Q(t)^2 I_{sne}}{q^2A^2\left[W_B - W_{bcj}(t)\right]^2 n_i^2} \qquad (4.29)$$

Chapter 5

Results & Discussion

The consequence of our work on NPT IGBT will be shown in this chapter. We have focused on the change of anode current, anode voltage and power loss due to rise of temparature in IGBT. These changes has been comapred with linear model. The simulations of these parameters has been done on MATLAB. Details of our work are given below-

5.1 Changes in Anode Voltage :

We had experimented the changes in anode voltage for different temparatures with respect to time. Mainly, voltage changes in accordance to carrier lifetime. As rising of temparature also hampers the carrier lifetime, so it changes the anode voltage. Below, difference between linear model and parabolic model is shown for different temparatures.

5.1.1 Low Carrier Lifetime : In the state of low carrier lifetime, voltage rises frequently with respect to time. In this case, the excess minority carrier removes and arrived at supply bus voltage (V_{bus}=400V) in a short time. So, voltage rise is faster but it changes with temparature rise.

At 27^o centigrade, we can see from FIgure 5.1.1 that voltage rises very fastly. In comapre with Hefnar's model, the rising time is almost same but the time to reach the top isdifferent. Our parabolic model shows faster rise in output anode current than the linear model.

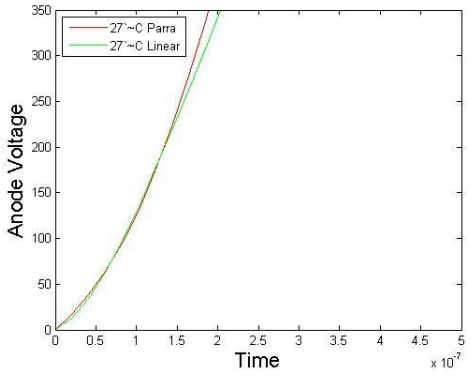

(a)

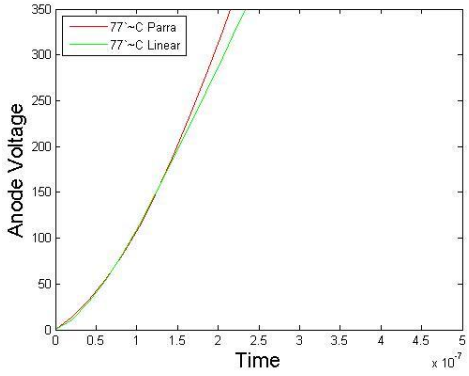

(b)

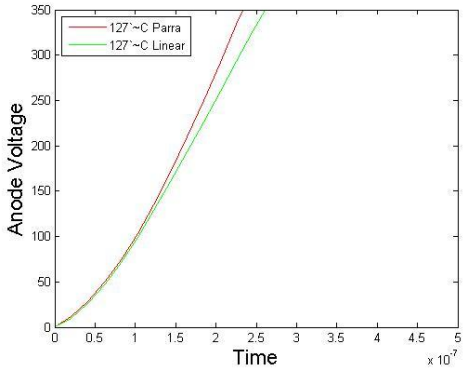

(c)

Figure-5.1.1:A comparison between parabolic model and linear modelfor the anode voltage for low carrier lifetime(Initial Carrier Lifetime, τHL= 0.5μs) for different temparature, (a)27°C, (b)77°C, (c)127°C

When temparature rises, voltage rising time also increases. As for rising temparature, carrier lifetime also increases a bit. As a result, it takes some more time for the charges to reach collector-base region, so transient anode voltage rising time increases. We can see in Figure 5.1.2, for this temparature, linear model shows a small deviation with parabolic model, that means parabolic model's performance for rising temparature is better than linear model.

5.1.2High Carrier Lifetime: When we consider high carrier lifetime, the affective base width becomes high than the diffusion lenght. As a result, the voltage rising time increases compare to low carrier lifetime condition. This increament also varies with temparature.

At 27°C, as for the characteristics of anode voltage, it requires less time for voltage to rise for parabolic model compared to linear model. As we can see from the below figure 5.1.4, for temparature rise, the anode voltage curve shift to right. In all the situation, linear curves always stays after parabolic one's. That means in parabolic model voltage rise time is bit less than linear model for all the temparature,

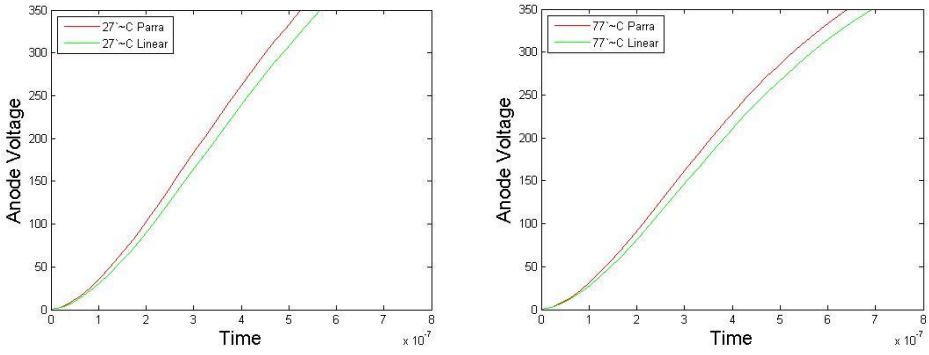

(a) (b)

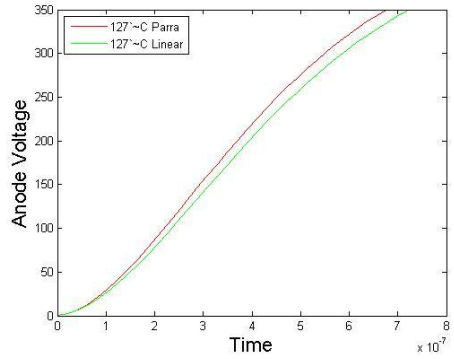

(c)

Figure 5.1.2: Difference between parabolic model and linear model for transient anode voltage for high carrier lifetime (Initial Carrier Lifetime, τ_{HL}= 7.1 μs) at 27ºC, 77ºC and 127ºC

From all the above figures and discussions, it is clearly seen that for both low and high carrier lifetime, parabolic model shows good agreement for device than linear model. So for anode voltage, our hypothesis supports parabolic model on top of linear model.

5.2. Changes in Anode Current: Anode current in IGBT is being affected by charge destribution in n- drift region and carrier lifetime of the charge. Anode current is directly proportional to carrier lifetime. In high carrier lifetime, anode voltage rise time increases than the low carrier lifetime, as a result, current decays slowly which indicates high anode current. In this situation, the anode current characteristics changes for temparature rise which are discussed below with figures.

5.2.1 Low Carrier Lifetime: When the carrier lifetime is low, it takes little time for the charges to be extracted. So, the current decay rate is slower than other carrier lifetime. It also changes with temparature. In 27ºC, the current decay rate is very high for both linear and parabolic model. Here, parabolic model tells very few current is flowing in IGBT in contrast to linear model. As temparature grows, charge decay rate becomes high, so current decay rate also goes high. In 77ºC and 127ºC, the minority carrier failed to reach to collector-base junction, so current decay rate rises and more current passes through the IGBT. But in case of linear model, less current in contrast to time is flowing through IGBT in parabolic model. In below figure, the changes has been showed in different temprature for transient anode current in low carrier lifetime.

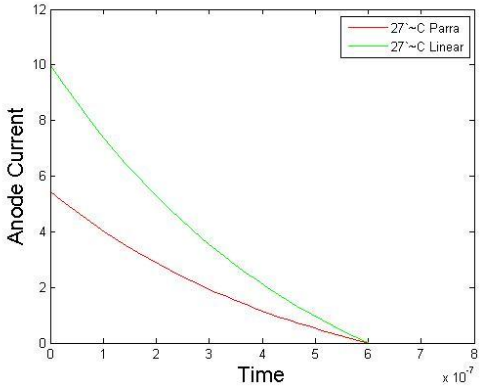

(a)

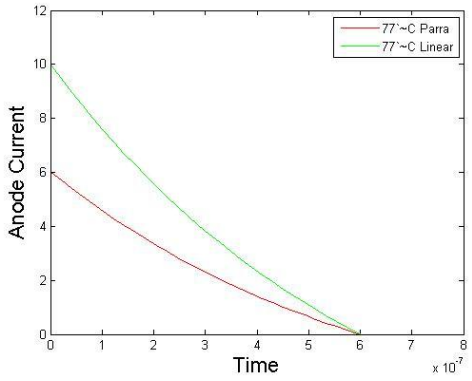

(b)

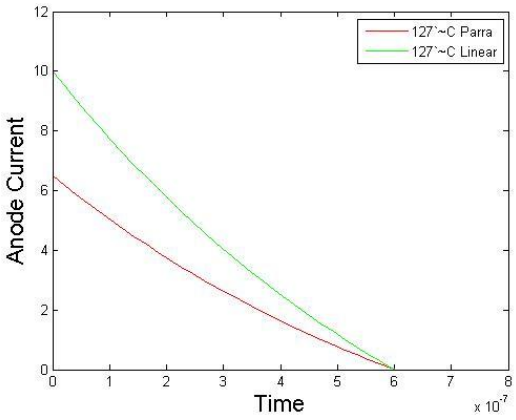

(c)

Figure-5.2.1:A comparison between parabolic model and linear modelfor the anode current for low carrier lifetime(Initial Carrier Lifetime, τ_{HL}= 0.5μs) for different temparature, (a)27°C, (b)77°C, (c)127°C

5.2.2 High Carrier Lifetime:For high carrier lifetime, the removal of minority carrier has increased. As the time for removal carrier rises, the anode voltage rise time also increases and as a result, high anode current passes through IGBT. From the below figure 5.2.2, we can see that the amount of current is became high than the lower carrier lifetime. For this, current decay rate also rises drastically.

As temparature rises, the amount of current changes as minority carrier concentration changes. The current increases and current decay rate increases in temparature rising. In 27°C, the parabolic model shows less decay in contrast to linear model. Same characteristics we can see in other two temparatures. In 77°C and 127°C, between parabolic and linear model, current decay rate is faster in linear model.

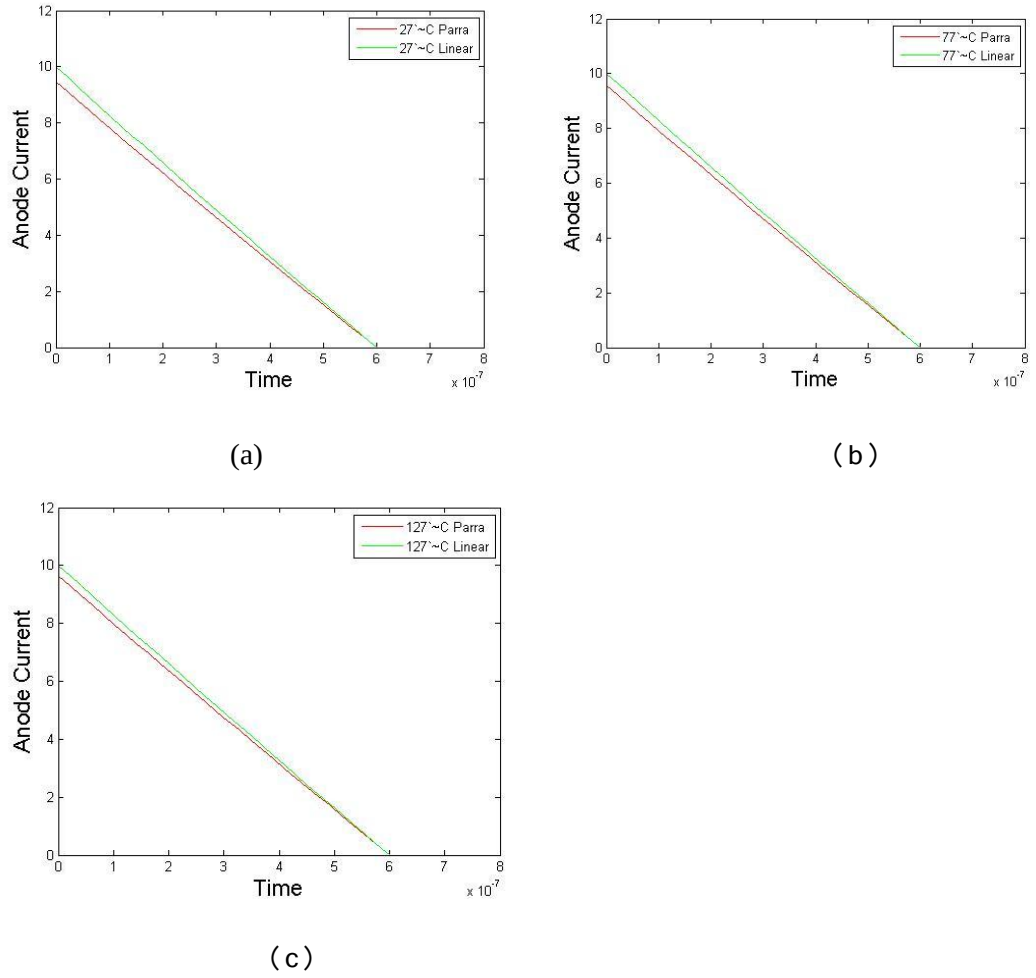

Figure-5.2.2:A comparison between parabolic model and linear modelfor the anode current for low carrier lifetime(Initial Carrier Lifetime, τ_{HL}= 7.1 μs) for different temparature, (a)27^{o}C, (b)77^{o}C, (c)127^{o}C

5.3. Changes in Switching Power Loss: Switching power loss in IGBT occurs during switch off period. This switch off action is controlled by MOSFET gate voltage of IGBT. When the IGBT is switched off, the gate voltage becomes less than threshold voltage, so electron current on MOSFET will stop flowing. In this case, the minority carriers which stored in n-drift region needs some time to be eliminated. During this time, IGBT has both anode current and anode voltage within it which produces power. This produced power can not be used anywhere rather it's becoming switching power loss of IGBT. We can get the swicthing power loss by multiplying anode voltage and anode current. The amount of power changes with change in minority carrier lifetime and temparature. Below, the changes in switching power for different carrier lifetime and temparature are showing with figures.

5.3.2 High Carrier Lifetime: In case of high carrier lifetime, the diffusion length, L is greater than the effective base width, W (W<L). For this, it takes more time for the minority carriers to be removed and holds greater current and voltage. As for temparature rise, the minority carrier lifetime increases, so the time to remove the charges also increases. As a result, power loss will high if the temparature is high.

Here, both linear and parabolic model showed much consistancy. The more carrier lifetime will increase, the ambipolar diffusion length will grow larger than the base width and parabolic model will be very much closer to linear model.

From the below figure 5.3.1, we can see that for 27°C, the power is high than the other temparatures and parabolic curve is very close to linear curve. When temparature rises to 77°C, the diffusion length becomes more large and parabolic model gradually forces the excess carrier concentration to the linear model and there is slight deviation between the two models. At 127°C, the larger diffusion length,L makes the parabolic model to be mostly matches to linear model.

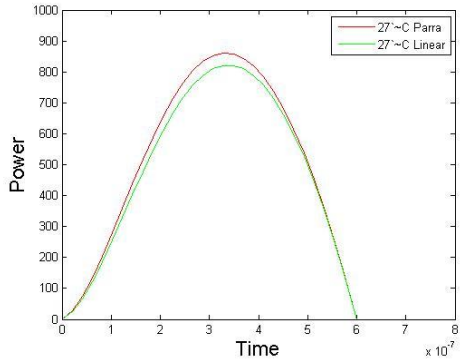

(a)

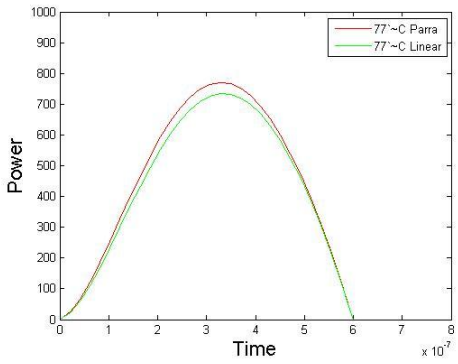

(b)

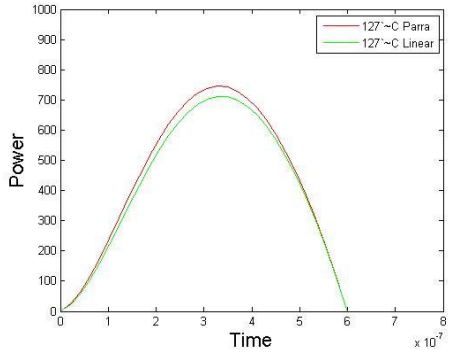

(c)

Figure 5.3.1 : A comparison between parabolic model and linear model
for the switching power loss for high carrier lifetime(Initial Carrier Lifetime, τHL= 7.1 μs) for different temparature, (a)27°C, (b)77°C, (c)127°C

5.3.2 Low Carrier Lifetime:When we consider low carrier lifetime, the effective base width, W is greater than ambipolar diffusion length, L (W>L). In this case, the current in parabolic model falls but the current decay rate is drastically down. For this, the deviation between parabolic model and li8near model is clearly seen.

From the below figure, we can see for 27^{o}C, the power is very high in contrast to high carrier lifetime. When the temparature rises, power for low carrier lifetime falls down. Here, parabolic model shows much consistancy than linear model and deviation between them is very high.

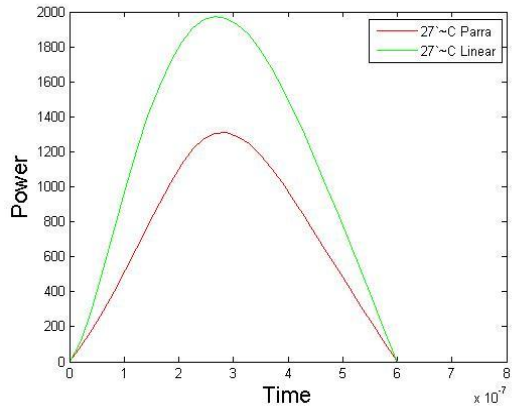

(a)

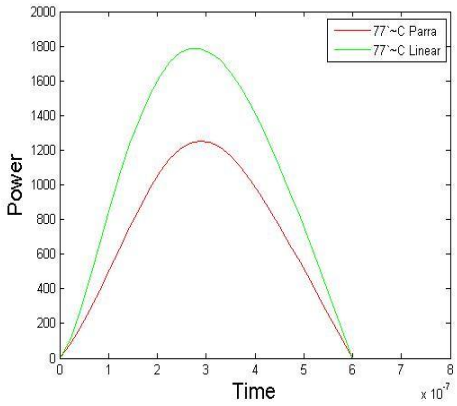

(b)

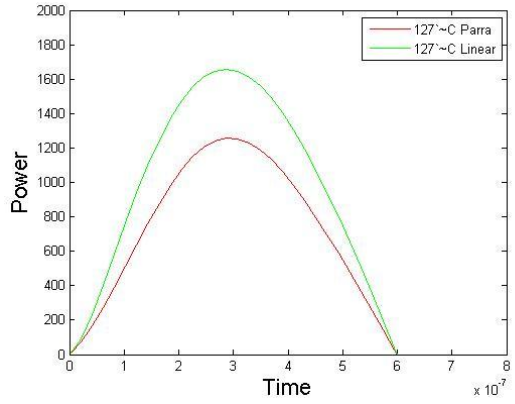

(c)

Figure 5.3.2 : A comparison between parabolic model and linear model
for the switching power loss for low carrier lifetime(Initial Carrier Lifetime, τHL= 0.5μs) for different temparature, (a)27^{o}C, (b)77^{o}C, (c)127^{o}C

Data Table:

For 0.5 μs –

Temperature (Degree)	Time(10^-7) (sec)	Current (A) (Parabolic)	Current (A) (Linear)	Voltage (V) (Parabolic)	Voltage (V) (Linear)	Power (W) (Parabolic)	Power (W) (Linear)
127	0	6.495	10	0	0	0	0
	1.436	4.273	6.857	176.55	160.7	754.4	1102
	2.872	2.614	4.248	479.34	390.1	1253	1657
	4.923	.813	1.272	678.062	628.5	551.4	799.7
	6	0	0	766.9	696.5	0	0
77	0	6.02	10	0	0	0	0
	1.436	4.004	6.682	190.2	184.6	761.6	1234
	2.872	2.429	4.04	517.4	442.6	1257	1788
	4.923	.747	1.171	787.3	693.4	588.3	812.1
	6	0	0	831.4	759.2	0	0
27	0	5.447	10	0	0	0	0
	1.436	3.501	6.428	222.4	218.5	778.8	1404
	2.872	2.041	3.747	641.4	524	1309	1964
	4.923	.5642	1.036	921	809.4	519.7	838.4
	6	0	0	980	890	0	0

For 7.1 μs –

Temperature (Degree)	Time(10^-7) (sec)	Current (A) (Parabolic)	Current (A) (Linear)	Voltage (V) (Parabolic)	Voltage(V) (Linear)	Power (W) (Parabolic)	Power (W) (Linear)
127	0	9.638	10	0	0	0	0
	1.436	7.283	7.557	52.17	46.54	380	351.7
	2.872	4.959	5.145	145.7	133.2	722.7	685.5
	4.923	1.791	1.755	271.8	255.5	459.7	448.3
	6	0	0	320	304	0	0
77	0	9.561	10	0	0	0	0
	1.436	7.214	7.545	55.27	48.26	398.7	367.2
	2.872	4.905	5.13	152.7	138.1	749.1	708.6
	4.923	1.669	1.749	282.2	263.3	471.1	459.6
	6	0	0	331	313	0	0
27	0	9.453	10	0	0	0	0
	1.436	7.117	7.529	61.74	53.63	439.4	403.8
	2.872	4.829	5.108	172.7	154.3	833.9	788.4
	4.923	1.638	1.733	328.3	303.4	537.9	525.9
	6	0	0	400	375	0	0

Chapter 6

Future opportunities

In our research paper, we have investigated the characteristics of NTP IGBT with temperature variance and deducted anode voltage, anode current and switching power in different carrier lifetime. We compared the extended parabolic model and linear model and analyzed the attributes with changing temperature. Although due to unavailability of practical data, we couldn't establish any preference of the compared models, we intend to research further on this area.

However, for a further approach, we can develop a PSPICE IGBT sub circuit for the parabolic model and examine I-V characteristics and study its switching features.

Moreover, as IGBT is a semiconductor device with integrated characteristics of power MOSFET and Bipolar junction transistor (BJT), it faces a notable power loss while switching which often results into hardware damage. To prevent the loss while turn-off and increase the efficiency of the device, we can determine the power loss approximately and develop the device to tolerate the circumstances.

References

[1] A. R. Hefner, \Analytical modeling of device-circuit interactions for the power insulated gate bipolar transistor (igbt)," IEEE Transactions on Industry Applications, vol. 26, no. 06, Nov-Dec 1990.
[2] A. R. Hefner and D. Blackburn, \An analytical model for the steady-state and transient characteristics of the power insulated-gate bipolar transistor," Solid-State Electronics, vol. 31, no. 10, pp. 1513-1532, 1988.

[3] B. J. Baliga, Power Semiconductor Devices. Boston: PWS publishers, 1996.

[4] A. Sattar, Insulated Gate Bipolar Transistor (IGBT) Basics, IXYS Corporation.

[5] M. Trivedi and K. Shenai, \Modeling the turn-off of igbts in hard and softswitching applications," pp. 887-893.
[6] A.Ramamurthy, S.Sawant, and B.J.Baliga, \Modeling the dv/dt of the igbt
Analysis of switching power loss in IGBT ; Page 73
during inductive turn-off."
[7] B. Fatemizadeh and D. Silber, \A versatile model for igbt including thermal effects," Seattle, USA, pp. 85-92.
[8] Y.Yue, J. Liou, and I.Batarseh, \A steady-state and transient model valid for all free-carrier injection conditions," 1997.
[9] J.Sgg, P. Tuerkes, and R. Kraus, \Parameter extraction methodology and validation for an electro-thermal physics-based npt igbt model," New Orleans, Louisiana, pp. 1166-1173
[10] D.S.Kuo, C.Hu, and S. Sapp, \An analytical model for the power bipolar mos transistor," pp. 1229-1237.
[11] K. Sheng, S. Finney, and B. Williams, \A new analytical igbt model with improved electrical characteristics," pp. 98-107.
[12] K. Sheng, B. Williams, and S. Finney, \A review of igbt models."
[13] P. Leturcq, \A study of distributed switching processes in igbts and other power bipolar devices," pp. 139-147.
[14] M. A. Hajji, \ A transient model for insulated gate bipolar transistors (igbts)," September 2002.
[15] V. K. Khanna, Insulated Gate Bipolar Transistor (IGBT) Theory and Design. 445 Hoes Lane, Piscataway, NJ 08854: IEEE Press, 2003.
[16] Patrick R Palmer, Enrico Santi, Jerry L Hudgins, Xiaosong Kang, John C Joyce, Yoon Eng, \Circuit Simulator Models for the Diode and Igbt with Full Temperature Dependent Features," 2003
[17] N. Thapar and J. B. Baliga, \An experimental evaluation of the on-state performance of the trench igbt designs."
[18] F. Udrea and G. Amartunga, \An on-state analytical model for the trench igbt."
Analysis of switching power loss in IGBT ; Page 74
[19] C. Y. Doo, Y. Kim, M. Han, and Y. Choi, \Numerical analysis of a new vertical igbt structure with reduced jfet effect."

[20] A. L. Robinson, D. N. Pattanayak, Adler, S. Michael, B. J. Baliga, and E. J. Wildi, \Lateral insulated gate transistors with improved latchup characteristics."
[21] M. Darwish and K. Board, \Lateral resurfed comfet," pp. 519-520.
[22] D. N. Pattanayak, A. Robinson, T. P. Chow, S. M. Adler, B. J. Baliga, and E. J. Wildi, \nchannel
lateral insulated gate transistors: Part i- steady- state characteristics," pp. 1956-1963.
[23] J. G. Fossum and Y. Kim, \Static and dynamic latchup in the ligbt," pp.1977-1985.
[24] M. Vellvehi, P. Godignon, D. Flores, J. Fernandez, S. Hidalgo, J. Rebollo, and J. Millan, \A new lateral igbt for high temperature operation," pp. 739-747.
[25] S. Ravishankar and B. J. Baliga, \Analysis of on-state carrier distribution in the di-ligbt," pp. 733-738.
[26] H. Qun and A. Gehan, \Forward blocking capability of double gate igbts at high temperatures," pp. 981-982.

Appendix A

Steady state charge control

Ambipolar Diffusion equation in Base

$$\frac{\partial^2 p(x)}{\partial x^2} - \frac{p(x)}{L^2} = 0 \qquad \text{(A.1)}$$

Boundary conditions:

$$p(x = 0) = P_0$$

$$p(x = W) = 0$$

Minority carrier concentration in n base region on IGBT is

$$p(x) = Ae^{\frac{x}{L}} + Be^{-\frac{x}{L}} \qquad \text{(A.2)}$$

Now at, $x = 0$

$$p(0) = A + B$$

$$P_0 = A + B \qquad \text{(A.3)}$$

Now at, $x = w$

$$0 = p(x) = Ae^{\frac{W}{L}} + Be^{-\frac{W}{L}} \qquad \text{(A.4)}$$

Now multiplying $e^{-\frac{W}{L}}$ to the equation (A.3), we get

$$Ae^{-\frac{W}{L}} + Be^{-\frac{W}{L}} = P_0 e^{-\frac{W}{L}} \qquad \text{(A.5)}$$

Subtracting (A.5) from (A.4), we get A

$$A\left(e^{\frac{W}{L}} + e^{-\frac{W}{L}}\right) = -P_0 e^{-\frac{W}{L}}$$

$$A = \frac{-P_0 e^{-\frac{W}{L}}}{2j\sinh\left(\frac{W}{L}\right)} \qquad \text{(A.6)}$$

Again we multiply equation (A.3) with $e^{\frac{W}{L}}$

$$Ae^{\frac{W}{L}} + Be^{\frac{W}{L}} = P_0 e^{\frac{W}{L}} \tag{A.7}$$

Subtracting (A.7) from (A.4), we find out B

$$B\left(e^{\frac{W}{L}} - e^{-\frac{W}{L}}\right) = P_0 e^{\frac{W}{L}}$$

$$B = \frac{P_0 e^{\frac{W}{L}}}{2j\sinh\left(\frac{W}{L}\right)} \tag{A.8}$$

So, the total solution would be

$$p(x) = \frac{-P_0 e^{-\frac{W}{L}}}{2j\sinh\left(\frac{W}{L}\right)} e^{\frac{x}{L}} + \frac{P_0 e^{\frac{W}{L}}}{2j\sinh\left(\frac{W}{L}\right)} e^{-\frac{x}{L}} \tag{A.9}$$

$$= P_0 \frac{e^{\frac{W-x}{L}} - e^{-\frac{(W-x)}{L}}}{2j\sinh\left(\frac{W}{L}\right)}$$

$$p(x) = P_0 \frac{\sinh\left(\frac{W-x}{L}\right)}{\sinh\left(\frac{W}{L}\right)} \tag{A.10}$$

Now, integrating p(x), we get the total steady state excess base charge

$$Q_0 = qA\int_0^W p(x)dx$$

$$Q_0 = qA\frac{P_0}{\sinh\left(\frac{W}{L}\right)}\int_0^W \sinh\left(\frac{W-x}{L}\right)dx$$

Let,

$$\frac{W-x}{L} = z$$

Differentiating

$$\frac{-1}{L}dx = dz$$

$$dx = -Ldz$$

Boundary Limits:

x=0 $z = \frac{W}{L}$

x=W $z = 0$

so,we get

$$Q_0 = qA\frac{P_0}{\sinh\left(\frac{W}{L}\right)}\int_{\frac{W}{L}}^{0}\sinh(-L)\sinh z dz$$

$$= \frac{qAP_0L}{\sinh\left(\frac{W}{L}\right)}[\cosh z]_0^{\frac{W}{L}}$$

$$= \frac{qAP_0L}{\sinh\left(\frac{W}{L}\right)}\left[\cosh\left(\frac{W}{L}\right) - 1\right]$$

We know,

$$\cosh(2x) = 1 + 2sinh^2\,(x) \qquad \text{(A.11)}$$

$$\sinh(2x) = 2\sinh(x)\cosh(x) \qquad \text{(A.12)}$$

The total excess base charge

$$Q_0 = qAP_0L\frac{2sinh^2\left(\frac{W}{2L}\right)}{2\sinh\left(\frac{W}{2L}\right)\cosh\left(\frac{W}{2L}\right)}$$

$$Q_0 = qAP_0L\tanh\left(\frac{W}{2L}\right) \qquad \text{(A.13)}$$

Appendix B

Linear Charge Control

From the steady state analysis, we have

$$p(x) = P_0 \frac{\sinh\left(\frac{W-x}{L}\right)}{\sinh\left(\frac{W}{L}\right)} \qquad \text{(B.1)}$$

Since the diffusion length (L) is larger than the drift layer thickness (W_B) because of the high lifetime of the carriers, one can approximate the carrier profile for the holes p(x) in the drift layer by a linear expression as shown previously

$$p(x,t) = P_0 \left[1 - \frac{x}{W(t)}\right] \qquad \text{(B.2)}$$

With the aid of the general ambipolar transport hole current expression

$$I_p = \frac{1}{1+b} I_T(t) - qAD \frac{\partial p(x)}{\partial x} \qquad \text{(B.3)}$$

We can find an expression for P_0 from equations (B.2) & (B.3) as

$$\frac{\partial p(x)}{\partial x} = -\frac{P_0}{W(t)} \qquad \text{(B.4)}$$

As

$$I_n(0) = 0$$

So

$$I_p(0) = I_T(t)$$

And

$$I_p(0) = I_T(t) = \frac{I_T(t)}{1+b} + \frac{2qAD_P}{1+\frac{1}{b}} \frac{P_0}{W(t)}$$

$$I_T(t)\left[1 - \frac{1}{1+b}\right] = \frac{2qAD_P}{1+\frac{1}{b}} \frac{P_0}{W(t)}$$

$$I_T(t) = I_T(t=0) = I_T(0^-)$$

$$P_0 = \frac{W(t)I_T(0^-)}{2qAD_P} \qquad \text{(B.5)}$$

Since total anode current is constant$I_T(t) = I_T(0^-)$, from the above equation we can find $\frac{\partial P_0}{\partial t}$ as

$$\frac{\partial P_0}{\partial t} = \frac{W(t)I_T(0^-)}{2qAD_P}\frac{d}{dt}W(t)$$

Substituting for $I_T(0^-)$ from equation (B.5), the above equation becomes

$$\frac{\partial P_0}{\partial t} = -\frac{P_0}{W(t)}\frac{d}{dt}W(t) \qquad \text{(B.6)}$$

From Figure (3.3) the slope is negative since the behaviour of $W(t)$ tends towards the minus x direction as the device voltage $V_{CE}(t)$ varies with time (moving boundary). The total excess charge in the base of the IGBT is

$$Q(t) = qAP_0 \int_0^W \left[1 - \frac{x}{W(t)}\right] dx$$

$$= qAP_0 \left[x - \frac{x^2}{2W(t)}\right]_0^W$$

$$= qAP_0 \left[W(t) - \frac{W(t)^2}{2W(t)}\right]$$

$$= qAP_0 \left[W(t) - \frac{W(t)}{2}\right]$$

$$= qAP_0 \frac{W(t)}{2} \qquad \text{(B.7)}$$

$$Q(t) = qA\frac{W(t)}{2}\frac{W(t)I_T(t)}{2qAD_P}$$

$$I_T(t) = \frac{4D_P}{W(t)^2}Q(t) \qquad \text{(B.8)}$$

Equation (B.8) is the linear charge control current and $W$is a constant in this case since $\frac{dV_{CE}}{dt} = 0$

Appendix C

Effective Depletion width from Poisson's Equation

[27] An electric field is created in the depletion region by the separation of positive and negative space charge densities. Fig. C.1 shows the volume charge density distribution in the pn junction assuming uniform doping and assuming an abrupt junction approximation. We will assume that the space charge region abruptly ends in the n region at $x = +x_n$,and abruptly ends in the p region at$x = -x_p$, (x_p is a positive quantity).

The electric field is determined from Poisson's equation which, for a one-dimensional analysis, is

$$\frac{d^2\emptyset(x)}{dx^2} = \frac{-\rho}{\epsilon_s} = -\frac{dE(x)}{dx} \qquad \text{(C.1)}$$

Where $\emptyset(x)$ is the electric potential, $E(x)$is the electric field, $\rho(x)$is the volume charge density and ϵ_s is the permittivity of the semiconductor. From Fig. D.1, the charge densities are

$$\rho(x) = -eN_a \qquad -x_p < x < 0 \qquad \text{(C.2)}$$

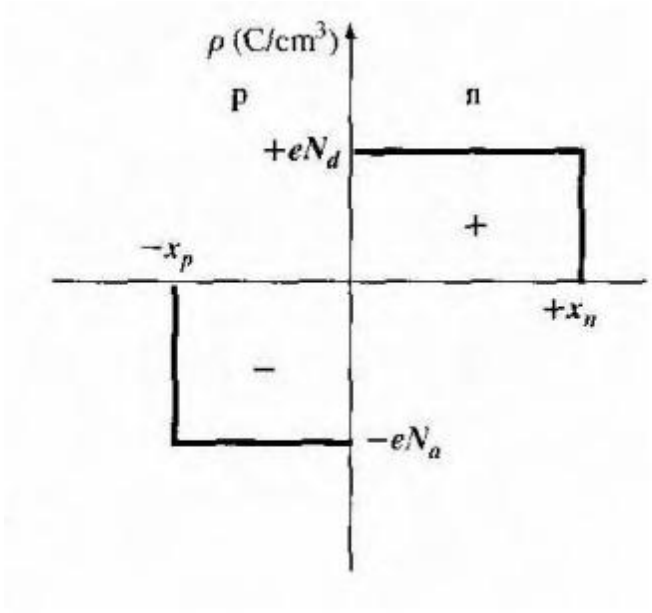

Figure C.1: The space charge density in a uniformly doped pn junction assuming the abrupt junction approximation

and,

$$\rho(x) = -eN_d \qquad 0 < x < x_n \qquad \text{(C.3)}$$

The electric field in the p region is found by integrating Equation (C.1), We have that

$$E = \int \frac{\rho(x)}{\epsilon_s} dx = -\int \frac{eN_a}{\epsilon_s} dx = -\frac{eN_a}{\epsilon_s} x + C_1 \qquad \text{(C.4)}$$

Where C_1 is a constant of integration. The electric field is assumed to be zero in the neutral p region for $x < x_p$, since the currents are zero in thermal equilibrium. As there are no surface charge densities within the pn junction structure, the electric field is a continuous function. The constant of integration is determined by setting
$E = 0$ at $x = x_p$. The electric field in the p region is then given by

$$E = -\frac{eN_a}{\epsilon_s}(x + x_p) \qquad -x_p \leq x \leq 0 \qquad \text{(C.5)}$$

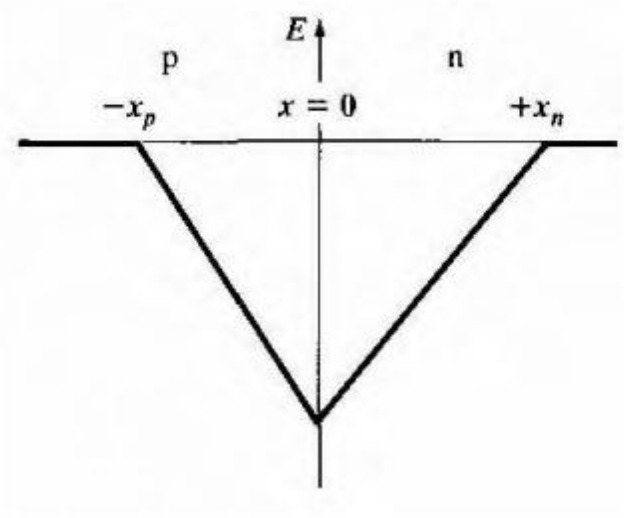

Figure C.2: Electric field in the space charge region of a uniformly doped pn junction

Then the n region, the electric field is determined from

$$E = \int \frac{eN_d}{\epsilon_s} dx = \frac{eN_d}{\epsilon_s} x + C_2 \qquad \text{(C.6)}$$

Where C_2 is again a constant of integration. The constant $C_2$is determined by setting $E = 0$ at $x = x_n$, since the Electric field is assumed to be zero in the n region and is a continuous function. Then

$$E = -\frac{eN_a}{\epsilon_s}(x_n - x) \qquad 0 \le x \le x_n \qquad \text{(C.7)}$$

The electric field is also continuous at the metallurgical junction, or at $x = 0$.Setting

Equations (C.5) and (C.7) equal to each other at $x = 0$ gives

$$N_a x_p = N_d x_n \qquad \text{(C.8)}$$

Equation (C.8) states that the number of negative charges per unit area in the p region is equal to the number of positive charges per unit area in the n region.

Fig. C.2 is a plot of the electric field in the depletion region. The electric field direction is from the n to the p region, or in the negative x direction for this geometry. For the uniformly doped pn junction, the Electric field is a linear function of distance through the junction, and the maximum (magnitude) electric field occurs at the metallurgical junction. An electric field exists in the depletion region even when no voltage is applied between the p and n regions.

The potential in the junction is found by integrating the electric field. In the p region then, we have

$$\emptyset(x) = -\int E dx = \int \frac{eN_a}{\epsilon_s}(x + x_p)dx \qquad \text{(C.9)}$$

$$\emptyset(x) = \frac{eN_a}{\epsilon_s}\left(\frac{x^2}{2} + x_p\right) + C_1' \qquad \text{(C.10)}$$

where C_1' is again a constant of integration. The potential difference through the pn junction is the important parameter, rather than the absolute potential, so we may arbitrarily set the potential equal to zero at $x = -x_p$. The constant of integration is then found as

$$C_1' = \frac{eN_a}{2\epsilon_s}{x_p}^2 \qquad \text{(C.11)}$$

so that the potential in the p region can now be written as

$$\emptyset(x) = \frac{eN_a}{2\epsilon_s}\left(x + x_p\right)^2 \qquad -x_p \le x \le 0 \qquad \text{(C.12)}$$

The potential in the region is determined by integrating the electric field in the n region, or

$$\emptyset(x) = -\int E dx = \int \frac{eN_d}{\epsilon_s}(x_n - x)dx \qquad \text{(C.13)}$$

Then

$$\emptyset(x) = \frac{eN_d}{\epsilon_s}\left(x_n x - \frac{x^2}{2}\right) + C_2' \qquad \text{(C.14)}$$

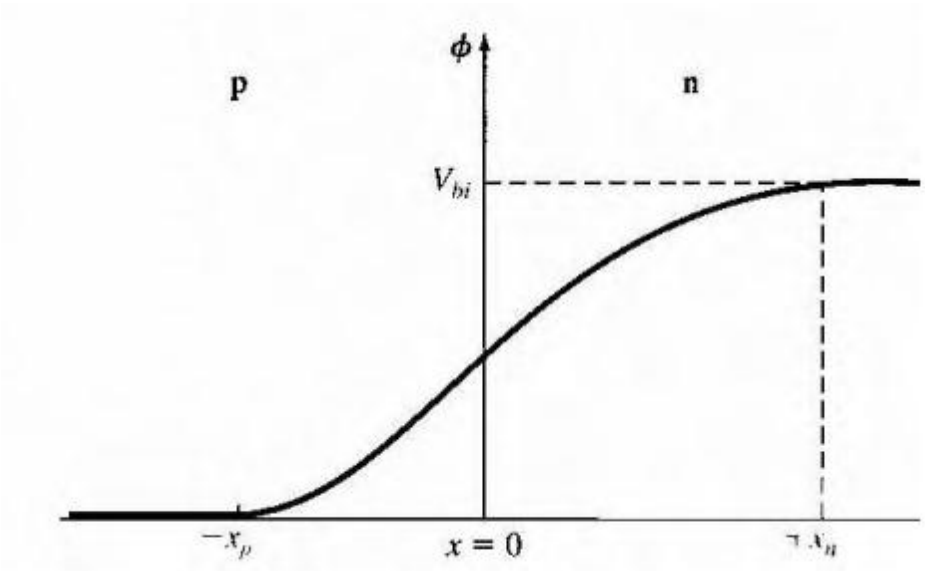

Figure C.3: Electric Potential through the space charge region of a uniformly doped pn junction

where C_2' is another constant of integration. The potential is a continuous function, so setting Equation (7.21) equal to Equation (C.14) at the metallurgical junction, or at x = 0, gives

$$C_2' = \frac{eN_a}{2\epsilon_s}x_p^2 \qquad \text{(C.15)}$$

The potential in then region can thus be written as

$$\emptyset(x) = \frac{eN_d}{\epsilon_s}\left(x_n x - \frac{x^2}{2}\right) + \frac{eN_a}{2\epsilon_s}x_p^2 \qquad 0 \le x \le x_n \qquad \text{(C.16)}$$

Fig. C.3 is a plot of the potential through the junction and shows the quadratic dependence on distance. The magnitude of the potential at $x = x_n$ is equal to the built-in potential barrier. Then from Equation (C.16), we have

$$V_{bi} = [\emptyset(x = x_n)] = \frac{e}{2\epsilon_s}\left(N_a x_p^2 + N_d x_n^2\right) \qquad \text{(C.17)}$$

We can determine the distance that the space charge region extends into the p and n regions from the metallurgical junction. This distance is known as the space charge width or Depletion Width. From Equation (C.8), we may write;

For example

$$x_p = \frac{N_d x_n}{N_a} \qquad \text{(C.18)}$$

Then, substituting Equation (C.18) into Equation (C.17) and solving for x, we obtain

$$x_n = \left\{\frac{2\epsilon_s V_{bi}}{e}\left(\frac{N_a}{N_d}\right)\left(\frac{1}{N_a+N_d}\right)\right\}^{\frac{1}{2}} \qquad \text{(C.19)}$$

Equation (C.19) gives the space charge width or the width of the depletion region, x_n,extending into the n-type region for the case of zero applied voltage.
Similarly, if we solve for x_n from Equation (C.8) and substitute into Equation (C.17), we find

$$x_p = \left\{\frac{2\epsilon_s V_{bi}}{e}\left(\frac{N_d}{N_a}\right)\left(\frac{1}{N_a+N_d}\right)\right\}^{\frac{1}{2}} \qquad \text{(C.20)}$$

Where x_p is the width of the depletion region extending into the p region for the case of zero applied voltage.

The total depletion or space charge width W is the sum of the two components, or

$$W_{depletion} = x_n + x_p \qquad \text{(C.21)}$$

Using Equations (C.19) and (C.20), we obtain

$$W_{depletion} = \left\{\frac{2\epsilon_s V_{bi}}{e}\left(\frac{N_a+N_d}{N_a N_d}\right)\right\}^{\frac{1}{2}} \qquad \text{(C.22)}$$

In case of collector-base region of the IGBT, the collector is highly doped p^+ region, whether the base is lightly doped n^-. So we can say $N_d << N_a$. From equation (C.8) we see

$$x_n >> x_p \qquad \text{(C.23)}$$

and

$$x_n \approx \mathrm{W_{bcj}} \qquad \text{(C.24)}$$

where $W_{bcj} = W_{depletion}$. Here V_{bi}=V_{CE} (collector-emitter voltage), q=e (electron charge) and N_d=N_b (base impurity concentration). So the base-collector depletion width reduces to

$$W_{bcj} = \left\{\frac{2\epsilon_s V_{CE}(t)}{qN_B}\right\}^{\frac{1}{2}} \qquad \text{(C.25)}$$

If the metallurgical base width is W_B, then the effective depletion width can be written as

$$W(t) = W_B - W_{bcj}(t)$$

$$W(t) = W_B - \sqrt{\left\{\frac{2\epsilon_s V_{CE}(t)}{qN_B}\right\}} \qquad \text{(C.26)}$$

Appendix D

Ambipolar Diffusion Coefficient

At high injection levels, electrons and holes transport cannot be treated separately because the electrons move in a cloud of holes and conversely. A convenient approach to handle this situation involves combination of continuity equation for electrons with that for holes, and introduction of a new parameter, namely, Ambipolar Diffusion Coefficient, which is an algebraic function of electron and hole diffusivities and concentrations. The defining equation for the ambipolar diffusion coefficient is

$$D = \frac{nq\mu_n D_p + pq\mu_p D_n}{nq\mu_n + pq\mu_p}$$

Where,

D_n =Electron Diffusion Coefficient

D_p = Hole Diffusion Coefficient

μ_n = Electron mobility

μ_p = Hole mobility

n = electron concentration

p = hole concentration

q = charge

The advantage gained from this approach is that the resulting single equation allows focusing our attention on the minority carrier concentration, while the presence of majority carrier concentration is automatically accounted for by the ambipolar diffusion coefficient.

Now, we know from Eienstein's Equation

$$\frac{D_n}{\mu_n} = \frac{kT}{q}$$

$$\frac{D_p}{\mu_p} = \frac{kT}{q}$$

$$\frac{D_n}{D_p} = \frac{\mu_n}{\mu_p} = b$$

Assuming $n = p$

$$D = \frac{nq(\mu_n D_p + \mu_p D_n)}{nq(\mu_n + \mu_p)}$$

$$= \frac{(\mu_n D_p + \mu_p D_n)}{(\mu_n + \mu_p)}$$

$$= \frac{\left(\frac{\mu_n}{\mu_p} D_p + D_n\right)}{\left(\frac{\mu_n}{\mu_p} + 1\right)}$$

$$= \frac{bD_p + D_n}{b+1}$$

$$= \frac{D_p + \frac{D_n}{b}}{1 + \frac{1}{b}}$$

$$= \frac{D_p + D_n \frac{D_p}{D_n}}{1 + \frac{1}{b}}$$

$$= \frac{2D_p}{1 + \frac{1}{b}}$$

So, $$D\left(1 + \frac{1}{b}\right) = 2D_p \qquad \text{(D.1)}$$

Appendix E

Fourth order RUNGE-KUTTA

(RK4) method

Fourth order Runge-Kutta (RK4) method is a numerical technique used to solve ordinary differential equation of the form:

$$\frac{dy}{dx} = f(x, y),\ y(0) = y_0$$

So only first order ordinary differential equations can be solved by using the Runge

- Kutta 4th order method.

The most commonly used set of values leads to the procedure:

$$y_{n+1} = y_n + \frac{1}{6}(k_1 + 2k_2 + 2k_3 + k_4)$$

$$k_1 = hf(x_n, y_n)$$

$$k_2 = hf\left(x_n + \frac{1}{2}h, y_n + \frac{1}{2}k_1\right)$$

$$k_3 = hf\left(x_n + \frac{1}{2}h, y_n + \frac{1}{2}k_2\right)$$

$$k_4 = hf(x_n + h, y_n + k_3)$$

The local error term for the fourth-order Runge-Kutta method is

$$(oh^4)$$

The global error would be

$$(oh^4)$$

It is computationally more efficient than the modified Euler method because, although four evaluations of the function are required per step rather than two, the steps can be many-fold larger for the same accuracy. The Runge-Kutta techniques have been very popular, especially the forth order method just presented. Because going from two to fourth order was so beneficial, we may wonder whether we should use a still higher order formula. Higher order (fifth, sixth and so

on) Runge-Kutta formulas have been developed and can be used to advantage in determining a suitable size for h. Still, Runge-Kutta methods of order greater than four have the disadvantage that the number of function evaluations that are required is greater than the order than the method, while Runge-Kutta method of order 4 require the same number of evaluations as the order.

It is important to keep in mind that there are three possible sources of error in numerical calculations, such as solutions to ordinary differential equations. The one we have discussed the most is truncation error, the error associated with the number of terms in a series, e.g. Taylor series. Other sources of error are round-off errors, which will always be present even if our method is exact, and original data errors, associated with not knowing the initial conditions or boundary conditions exactly [see Box 3.1]. Errors at each step propagate through the solution, so the global error is generally about an order larger than the local error. A method is convergent if the approximate solution tends toward the true solution as

$$\Delta x \to 0$$

All of the widely used methods for solving ordinary differential equations (in particular the ones we have discussed) are convergent. Stability refers to the growth of errors as the solution proceeds. A stable method is one in which the global error does not grow in an unbounded manner. For many ODE's, the step size required to obtain an accurate solution is much smaller than the step size required for stability. As a result, stability is often not a major concern. When a solution is unstable, it is usually obvious. A smaller step size will generally rectify the problem, although there are cases that are unconditionally unstable for some methods. Changing methods is the best approach in such cases.